ELSEVIER

Polymer 43 (2002) 6609–6626

polymer

www.elsevier.com/locate/polymer

Role of entanglement in crystalline polymers 1. Basic theory

Kazuyoshi Iwata

Department of Applied Physics, Fukui University, Bunkyo 3-9-1, Fukui 910-8507, Japan

Received 31 May 2002; received in revised form 5 July 2002; accepted 5 July 2002

Abstract

When stacked lamellar crystals are formed in melts, entanglements are trapped and condensed in amorphous domains (a-domains); this makes the free energy of the a-domains increase and inhibits crystallization, thus, determines the crystalline structure of the system. Based on the local-knot (LK) model of entanglement proposed by Iwata and Edwards, the entanglement state of the system is described by three parameters, condensation ratio χ, trapping ratio ξ and average number $\bar{\nu}$ of LKs trapped per stem in the a-domains. It is shown that crystallinity w_c, average lamellar thickness $\bar{L}_c$ and average a-domain thickness $\bar{L}_a$ are written in terms of χ, ξ and $\bar{\nu}$ alone; this means that *structure of stacked lamellar crystals is determined by entanglement*. Particularly, the microscopic structure is determined by how LKs are partitioned in the stems of the a-domains. The equilibrium amorphous ratio in the limit $M \to \infty$ (which is called 'limiting equilibrium amorphous ratio $\hat{w}_a^{\infty}$') is a universal function of a reduced degree of supercooling, $\tau = (N_c \Delta h_m / k_B T_m^0)\Delta T/T$, where Δh_m is the enthalpy of fusion and N_c is the critical chain length of the entanglement transition; this means that $\hat{w}_a^{\infty}(\tau)$ is independent of polymer species, thermal history or morphological properties of the system. Based on this result, a method is proposed to determine trapping ratio ξ experimentally. Magnitudes as well as T- and M-dependence of w_c, $\bar{l}_c$ and $\bar{l}_a$ predicted by the theory agree reasonably with experiments. It is shown that the topological free energy of entanglement accumulated in the a-domains plays an important role in the melting phenomena: For example, folding surface energy σ_e changes largely from that estimated by the usual Thompson–Gibbs equation, and the abnormal increase of σ_e with increasing M in stacked lamellar crystals, the phenomenon found by Schultz and Manderkern, is explained by the accumulated topological energy. Mechanism of trapping LKs in the crystallization process is discussed in detail. © 2002 Published by Elsevier Science Ltd.

Keywords: Role of entanglement in crystalline polymers; Topological theory of crystalline polymers; Local–knot model

1. Introduction

Semi–crystalline polymers usually have periodical stacked lamellar structures of amorphous and crystalline domains (which are hereafter called a- and c-domains). These structures depend critically on the crystallization condition, such as the quenching rate, crystallization temperature and pressure, and also on detail microscopic properties of polymers such as molecular weight, tacticity, branching and so on. By recent developments of experimental techniques, a large amount of evidences have been accumulated that support this picture of semi–crystalline polymers [1–3]. However, many fundamental questions have not yet been answered.

(1) Why polymer chains should fold themselves in forming lamellar crystals?
(2) How structure of semi-crystalline polymers, such as crystallinity w_c, a-domain thickness l_a, c-domain thickness l_c and so on, are determined?
(3) How nucleation of crystallization occurs?
(4) Are a-domains different from the ordinary melts?

I believe that entanglement should play central roles in these problems.

The role of entanglement in crystalline polymers has been discussed by Manderkern [1,2]. Polyethylene, for example, is fully crystallized for molecular weight below $M \approx 10^4$ but, as M increases beyond it, w_c decreases and approaches to a limiting value $w_c = 0.25–0.3$ (in the case of isothermal crystallization). Mandelkern [1,2] argued that entanglements (such as knots, links or other topological analogues) existing in the initial melts are unknotted in the process of crystallization of low-molecular-weight polymers, so that their w_c approaches unity; as M increases, however, unknotting of entanglements becomes more difficult and they are trapped in a-domains and block thickening of the lamellae; the upper limit of w_c appears

E-mail address: iwata@polymer.apphy.fukui-u.ac.jp (K. Iwata).

0032-3861/02/$ - see front matter © 2002 Published by Elsevier Science Ltd.
PII: S0032-3861(02)00524-4

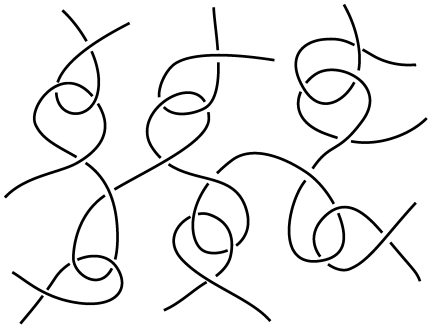

Fig. 1. Local-knot model.

when the all entanglements are trapped. Another closely related phenomenon is the reversible change of lamellae, in which w_c, l_c and l_a changes reversibly with changing T below crystallization temperature T_c [4–6]. Several different models are proposed for this phenomenon [6]: (1) reversible melting and re-crystallization of the surface of lamellae, (2) reversible formation and melting of new crystallites (the so-called second crystallization) and (3) reversible lattice distortion in the lamellae. Recently, Albrecht and Strobl [6] studied this phenomenon in polyethylene using the small-angle X-ray scattering and delatometry method and found that l_c increases with decreasing l_a but neither new formation of crystallites nor distortion of their lattice structure occur by cooling below T_c. From these results, they concluded that the reversible change of w_c should come from the first mechanism (surface melting of lamellae). Theoretical treatments of the surface melting phenomena are given by Fisher [7], Mansfield [8,9] and Strobl [6] based on trapped entanglements in the amorphous domains. According to them, chains are pulled out from the a-domains to thicken the lamellae as the system is cooled below T_c; in this process, the trapped entanglements are deformed to increase the free energy of the a-domains; w_c is determined by the balance between the chemical potentials of elements in the a- and c-domains. These two phenomena come from the same origin, trapped entanglements in the a-domains: What considered by Manderkern [1,2] is the M-dependence of w_c while that discussed by Fisher [7], Strobl [4–6] and Mansfield [8,9] is the T-dependence of w_c, but these phenomena should be discussed consistently using the same model and theory.

Role of entanglement in fiber drawing process is well known: drawing of polymer solutions and melts is possible only when chains are well entangled with each other; otherwise, strings cannot keep their form in the drawing process. This mechanism is particularly important in the ultra drawing method (gel drawing method) developed in 1980s [10,11]; in this technique, gels made from dilute solutions of high molecular weight polymers are drawn hundred times as long to form a super strong fiber with nearly perfect crystalline structure [10]. It is found that the rigidity of the fiber is linearly proportional to the maximum extension ratio, which is eventually inversely proportional to the square root of concentration c of the original solutions. This result is interpreted that the maximum extension ratio (and hence the rigidity of the fiber) is determined by entanglement spacing $M_e(c)$ of the original solutions [11]. In the drawing process, entanglements play a positive and negative role: the positive role is that entanglements keep a form of string in the drawing process; the negative role is that they remain as defects and reduce strength of the fiber. In any way, entanglements control the process of crystallization and determine the final structure of crystals formed. This must be the same in the all kinds of crystalline polymers including single crystals formed in dilute solutions, stacked lamellar crystals formed in melt and fiber crystals formed by drawing.

Although there are these discussions, they are still hypothetical and the role of entanglement in crystalline polymers is not recognized well. This may be due to that the present standard model of entanglement (the reptation/tube model [12]) is not sufficient for these problems. The reptation/tube model has been successfully applied to many dynamic problems of entanglement, such as viscoelasticity and diffusion of polymers [12]. However, it neglects topological features of entanglement, particularly the 'topological repulsive forces among local-knots (LKs)', which will play central roles in crystalline polymers as shown in this work. By nature, entanglement is a matter of topology and the role of entanglement in crystalline polymers will be understood only in its topological framework.

Local-knot model. Based on a topological consideration, Iwata and Edwards [13,14] proposed 'a local-knot model', in which entanglement is assumed to be composed of elementary units called LKs, which are formed among local-chains (local parts of chains of length ca. N_e, the average chain length per entanglement) as shown in Fig. 1. When a pair of local-chains forms an LK, its Gauss integral takes near integer number ± 1, ± 2,..., and keep its state until it moves to the end of the chains and unfastened. It is predicted that LKs move like one-dimensional Brownian particles along chains, interacting repulsively with one another and, in a long-time scale, they take part in a corrective motion which is assigned to the reptation motion [15]. These behaviors of LKs are later confirmed by computer simulations [17]. Although LKs cannot be observed directly by experiments, they should be considered as real physical entities since they are observed clearly by the computer simulations [16,17]. LK model is consistent with the reptation model in their dynamic behavior [15] but it has many novel features, such as the topological repulsive potential among LKs, which plays central roles in crystalline polymers. For example, the surface melting phenomenon is studied theoretically by Mansfield [8,9] using the slip-link model (in which the topological repulsive force is neglected), but it cannot explain the change of the free energy due to condensation of entanglements found in the previous work [17]. A similar condensation of

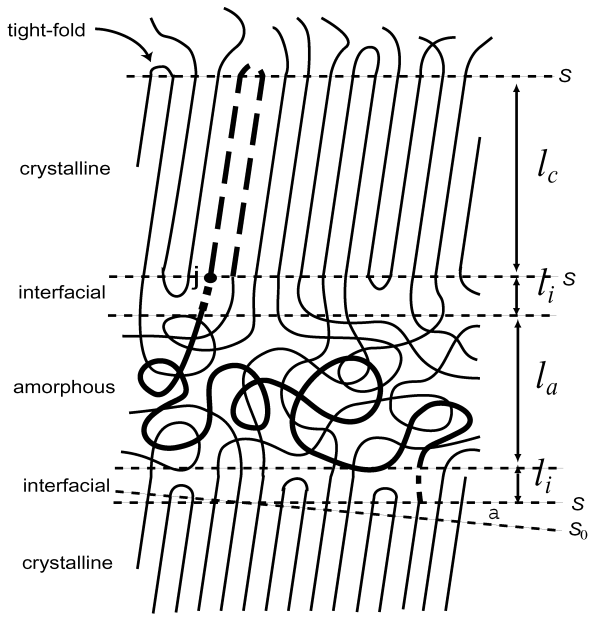

Fig. 2. Structure of stacking lamellar crystal.

entanglements occurs in the a-domains of stacked lamellar crystals and controls the crystallization process and structure of the crystals formed. These phenomena are explained only by topological models of entanglement, such as LK model.

In this series of works, various problems of crystalline polymers, such as (1)–(4) stated in Section 1, will be studied using LK model. These problems have been already discussed in the Symposium on Macromolecules of the Society of Polymer Science, Japan [20–23]. As an introduction to these works, the second problem, "How the structure of semi-crystalline polymers, such as w_c, l_c and l_a, are determined?", is discussed in this paper. The other works will be given in later series.

2. Local-equilibrium between amorphous and crystalline domains

Crystalline polymers are usually frozen in non-equilibrium states but, when stacked lamellar crystals are annealed for a sufficient long time, they approach to a local-equilibrium state between a- and c-domains. Although the local-equilibrium state is different from the true equilibrium state (the extended-chain crystalline state), the thermodynamic equilibrium condition can be applied between the a- and c-domains. We consider such systems as a standard state of stacked lamellar crystals. Stacked lamellar crystals are formed in various ways: they are usually obtained by cooling melt polymers but similar stacked structures are formed by rearrangement of isolated single lamellar crystals; there may be different kinds of stacked lamellar crystals which require different theoretical approaches. As an introduction, we consider here well-annealed stacked lamellar crystals formed from melts in the usual way. Non-annealed systems are also considered briefly but their detailed discussion will be given in future works.

The system considered here is composed of a- and c-domains of thickness l_a and l_c, staking periodically as shown in Fig. 2. In the figure, S represents a surface of a lamellae (c-domain), S_0, a plane perpendicular to the chain-axis of the lamellae and α, the tilt angle between S and S_0. Between the a- and c-domains, there are interfacial (i)-domains in which the ordered structure of the c-domains dissipates continuously to the random structure of the a-domains. We call such parts of a chain that pass the a-, c- and i-domains, a-, c- and i-sections of the chain, respectively; in Fig. 2, the a-, c- and i-sections are shown by straight, broken and dotted bold lines, respectively. Let L_a, L_c and L_i be the chain-length (in the unit of chain units) of the a-, c- and i-section. For convenience, c-sections connected by tight-folds on the folding surface are treated as single c-section (see Fig. 2) but the length of tight-holds is neglected for simplicity in the calculation of L_c. Tight-folding ratio φ_f (the ratio of chains coming out and returning immediately to an adjacent position on the folding surface of the lamellae) is rather small, say, $\varphi_f \leq 0.3$ for polyethylene, so that the c-sections contain no or, at most, few tight-folds.

In this work, we consider stacked lamellar crystals formed of very long chains, each of which passes the a-, c- and i-domains many times, say ten to hundred times. If chain ends appear uniformly in the a-, c- and i-domains, the total number of a- and c-sections, n_a and n_c, must be the same and the total number of i-sections, n_i, twice of them. Actually, the distribution of the chain-ends may not be uniform but we do not know which of the three domains the chain ends mainly appear. In any way, chain ends may be neglected in the sufficiently long chains as considered here, so that the simplest possible condition, $n_a = n_c = n_i/2$, may be assumed. In this case, we may consider that the system is composed of aici-sequences (sequences of a-, i-, c- and i-section shown by a bold-straight, dotted, broken and dotted lines in Fig. 2) and assume

$$\rho_a \bar{l}_a/\bar{L}_a = \rho_c \bar{l}_c/\bar{L}_c = \rho_i \bar{l}_i/\bar{L}_i = M_0 n(1-\varphi_f)\cos\alpha/N_A, \quad (2.1)$$

where $\bar{L}_a$, $\bar{L}_c$ and $\bar{L}_i$ are the *number* average of L_a, L_c and L_i, $\bar{l}_a$, $\bar{l}_c$ and $\bar{l}_i$, the *number* average of l_a, l_c and l_i, ρ_a, ρ_c and ρ_i, the density of the a-, c- and i-domains, n, the number of chains per unit area of surface S, and M_0, the molecular weight per chain unit. For short chains, Eq. (2.1) should be corrected for chain-ends but such chain-end effects are discussed in future works.

Now, let us consider how entanglements existing in the initial melt are trapped in the crystallization process. Following LK model, we assume that entanglement of polymer chains is composed of elementary units called LKs. In the equilibrium melt, an aici-sequence contains $\bar{\nu}^0 = (\bar{L}_c + \bar{L}_a + 2\bar{L}_i)/L^0_{LK}$ LKs as an average, where L^0_{LK} is the average chain length per LK in the topological equilibrium state. During crystallization and annealing, a part of LKs is

Table 1
Basic parameters of BF model and polyethylene

BF model ($\phi = 0.5$)[a]
$N_e = 89$
$N_c = 170$
$L_{LK} = 63$
Polyethylene
$\rho_c = 1.000$
$\rho_a = 0.855$
$\Delta h_m = 4.1$ kJ/mol
$T_m^0 = 141.4$ or 145.5 °C
$n = 5.48\ \mathrm{nm}^{-2}$
$N_e = 89.3$ (in CH_2)
$N_c = 271$ (in CH_2)

[a] Data for BF model are given in Refs. [17,18].

unknotted so that $\bar{\nu}^0$ decreases to $\bar{\nu} = \xi\bar{\nu}_0$, where ξ is the ratio (trapping ratio) of LKs remaining unsolved. We assume that trapped LKs are all condensed in the a-domains (or they do not enter in the i-domains), because the i-domains have a similar high-density as the c-domains (i.e. $\rho_i \approx \rho_c > \rho_a$). Relative condensation ratio χ of LKs in the a-domains is defined by

$$\chi = \xi(\bar{L}_a + \bar{L}_c + 2\bar{L}_i)/\bar{L}_a. \tag{2.2}$$

By definition, χ is equal to unity in the equilibrium melt. If a considerable part of LKs enters into the i-domains, Eq. (2.2) should be modified; however, Eq. (2.2) must be a rather good approximation in a low or medium supercooling condition where the amount of the i-domains is small, say, 5–15% of the total volume in polyethylene.

In the previous work [17], chemical potential μ of chain-elements was computed as a function of χ by computer simulations of catena networks (permanently entangled cyclic polymers), which is considered as a model of the a-domains. In the simulations, systems are equilibrated with an external element-bath of chemical potential μ by a hypothetical element exchange reaction under the restriction that entanglement among the chains is conserved. The catena network represents the a-domains and the element-bath, the c-domains of the stacked lamellar crystals. The simulation was done using the bond-fluctuation (BF) model at volume fraction $\phi = 0.5$. Chemical potential of chain elements (repeating units of BF model) relative to its equilibrium melt value was computed numerically and the result is fitted by [17]

$$\Delta\mu_{BFM}(\chi) = 0.03963 - 0.0369\chi + 0.00199\chi^2 - 0.00472\chi^3, \tag{2.3}$$

which is transformed into the free energy per element as follows [17]:

$$\Delta f_{BFM}(\chi) \equiv -\chi\int_1^\chi \chi'^{-2}\Delta\mu_{BFM}(\chi')\mathrm{d}\chi' = 0.03963 - 0.0400\chi + 0.0369\chi\ln\chi - 0.00199\chi^2 + 0.00236\chi^3. \tag{2.4}$$

In these equations, $\Delta\mu_{BFM}(\chi)$ and $\Delta f_{BFM}(\chi)$ are given relative to their topological equilibrium (melt equilibrium) values; thus $\Delta\mu_{BFM}(1) = 0$ and $\Delta f_{BFM}(1) = 0$ by definition. The catena network used in the simulations is different from the a-domains in the following two points: (1) chain elements in the a-domains are transferred through junction point j on the lamellar surface S (see Fig. 2), while they are added or removed randomly at any point of the chains in the simulation and (2) the terminal points (junction points) of the a-sections are fixed to the lamellar surfaces, while no element is fixed to the cell-walls in the simulation. As for the first point, $\Delta\mu_{BFM}(\chi)$ and $\Delta f_{BFM}(\chi)$ are exactly the same whether elements are added or removed at a few selected points (say, the junction points) or at any point of the chains, so long as the system is well equilibrated. As for point 2, the effect of fixed junction points may be neglected if $\bar{\nu}$, the average number of LKs per a-section is sufficiently larger than unity; in the systems considered here, $\bar{\nu}$ is in the range of few to hundreds as shown later so that this condition is roughly satisfied. Thus, the catena network used in the previous work [17] must be a good model of the a-domains.

To apply Eqs. (2.3) and (2.4) to real systems, $\Delta\mu_{BFM}(x)$ and $\Delta f_{BFM}(x)$ must be converted into $\Delta\mu_a(\chi)$ and $\Delta f_a(x)$ of the real polymers. Considering that $\Delta\mu_{BFM}(x)$ and $\Delta f_{BFM}(x)$ come from the topological repulsion among LKs, conversion is done by comparing N_e, the average entanglement spacing, or N_c, the critical chain length of the entanglement transition. There is, however, a problem in these indexes: according to the universality hypothesis of entanglement, ratio N_c/N_e should be constant but actually it changes between 1.7 and 3 among polymers [18,19]. In the most polymers the ratio is near two but polyethylene, which is considered mostly in this work, has an unusually high ratio $N_c/N_e = 3.0$. It is, therefore, a serious problem which of N_e and N_c should be used in converting $\Delta\mu_{BFM}(\chi)$ and $\Delta f_{BFM}(\chi)$ into $\Delta\mu_a(\chi)$ and $\Delta f_a(\chi)$ of polyethylene. This problem was discussed in the previous papers [18,19], where we argued that N_c is more reasonable than N_e as the index of entanglement, but it is still open to question. Therefore, we consider two conversion factors for N_e and N_c,

$$C_e = N_e(\text{real chain})/N_e(\text{BF model}), \tag{2.5}$$

$$C_c = N_c(\text{real chain})/N_c(\text{BF model}). \tag{2.5'}$$

$C(= C_e \text{ or } C_c)$ represents that each element of BF model corresponds to C repeating units of a real chain. With the

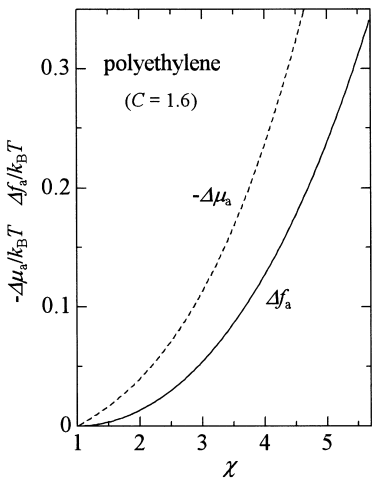

Fig. 3. $\Delta\mu(\chi)$ and $\Delta f(\chi)$ of polyethylene ($C = 1.6$).

use of C, $\Delta\mu_a(x)$ and $\Delta f_a(x)$ are given by

$$\Delta\mu_a(\chi) = k_B T \Delta\mu_{BFM}(\chi)/C,$$
$$\Delta f_a(\chi) = k_B T \Delta f_{BFM}(\chi)/C. \tag{2.6}$$

For polyethylene, C is estimated to be $C_e = 1.00$ or $C_c = 1.6$ using parameters given in Table 1. Thus, $\Delta\mu_a(\chi)$ and $\Delta f_a(\chi)$ of polyethylene computed for $C_c = 1.6$ are 60% larger than those estimated by $C_e = 1.00$; this discrepancy is a serous problem in comparing the theory with experiments. $\Delta\mu_a(\chi)$ and $\Delta f_a(\chi)$ computed for $C_c = 1.6$ are plotted against χ in Fig. 3. As seen from the figure, $\Delta f_a(\chi)$ takes minimum at $\chi = 1$, $\Delta\mu_a(\chi)$ decreases with increase in χ and becomes zero at $\chi = 1$. By definition, $\Delta\mu_a(\chi)$ represents the work necessary to pull a chain in the a-domain by one element into the equilibrium melts, thus it represents tensile force acting along the chains. The force, which is called the 'topological tensile force', comes from the topological repulsion among LKs and is different, in its origin as well as in its nature, from the 'tensile force of tube' assumed in the Doi–Edwards theory [12]. When the local-equilibrium between the a- and c-sections is established,

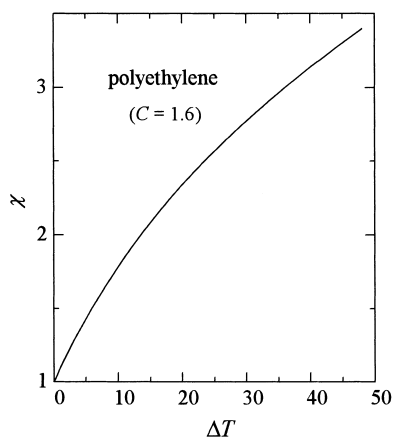

Fig. 4. χ computed as a function of ΔT ($= T_m^0 - T$) for polyethylene ($C = 1.6$).

χ and $\Delta\mu_a(\chi)$ should become constant in all a-sections in the system. Number ν of LKs trapped in each a-section is determined statistically as a chain is integrated into the lamellae in the growing front (this process is discussed in Section 5); once ν is determined, it is kept constant unless the lamellae melt. Even if ν is constant in each a-section, χ and $\Delta\mu_a(\chi)$ become the same in the all a-sections in the annealing process, where the a- and c-sections adjust their lengths and positions along the chain by sliding motion in the lamellae. If there is an imbalance of $\Delta\mu_a(\chi)$ in two a-sections connected to a c-section, it slides along the chain to reduce the imbalance until χ and $\Delta\mu_a(\chi)$ become the same in the all a-sections. This condition (equilibration of χ and $\Delta\mu_a(\chi)$ in the all a-sections) is a basic requirement for the local-equilibrium to be established.

Now, free energy $\Delta F(\chi, T)$ per aici-sequence is given by

$$\Delta F(\chi, T) = \bar{L}_c \Delta\mu_c(T) + \bar{L}_a \Delta f_a(\chi) + 2\hat{\sigma}_e/(1 - \varphi_f), \tag{2.7}$$

where $\Delta\mu_c(T)$ is the chemical potential of element in the c-domains relative to that of the equilibrium melt and $\hat{\sigma}_e$, the interfacial energy per stem on the folding surface. For a moderate supercooling, $\Delta T = T_m^0 - T$, $\Delta\mu_c(T)$ is given by

$$\Delta\mu_c(T) = -\Delta h_m \Delta T/T_m^0, \tag{2.8}$$

where Δh_m is the enthalpy of fusion per element. $\hat{\sigma}_e$ is not necessary constant but may change with χ (since tensile force $\Delta\mu_a(\chi)$ is acting on the surface of the lamellae). However, such dependence of $\hat{\sigma}_e$ on χ must be rather small, at least for small ΔT, so that we assume for simplicity that $\hat{\sigma}_e$ does not change during the local-equilibration process. Under this condition, the local-equilibrium state is determined by condition $\partial\Delta F(T, \chi)/\partial\bar{L}_c = 0$ with $\bar{L}_c + \bar{L}_a =$ const, which gives

$$\Delta\mu_c(T) = \Delta\mu_a(\chi). \tag{2.9}$$

This equation determines χ as a function of T. $\chi(T)$ thus computed for polyethylene is plotted against ΔT in Fig. 4 ($C = 1.6$ assumed). Since Eq. (2.9) represents a general phase-equilibrium condition, it should hold even if σ_e change in the annealing process. To show this, however, we must know the exact structure of the interfacial domains but this is out of the scope of this work.

3. Crystallinity ϕ_c and trapping ratio ξ of LKs in well-annealed systems

Crystallinity is usually defined as the volume faction of the c-domains

$$\phi_c = \bar{l}_c/(\bar{l}_a + \bar{l}_c + 2\bar{l}_i), \tag{3.1}$$

which is determined by various methods, such as the thermometric, delatometric, NMR, IR and Raman spectroscopic methods [1–3]. By the thermometric method, ϕ_c is determined, by the delatometric method, the sum of volume fraction of the c- and i-domains, $\phi_c + \phi_i$, is obtained and by

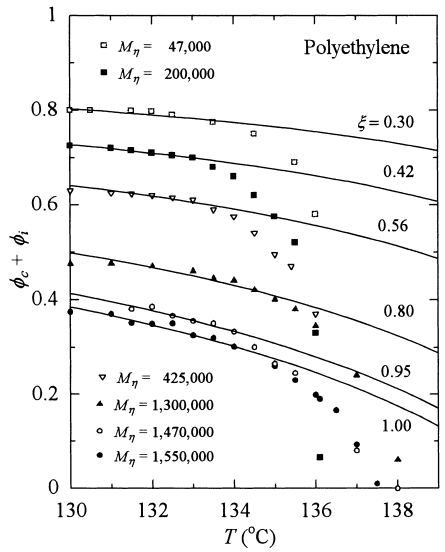

Fig. 5. T-dependence of $\phi_c + \phi_i$ of polyethylene ($M_\eta = 4.7–155 \times 10^4$) measured by Futou and Manderkern [24]. The samples are isothermally crystallized at $T = 130$ °C and never cooled below T_c. The experimental points are fitted by theoretical curves (straight lines, $C = 1.25$) with ξ as an adjustable parameter.

the spectroscopic methods, ϕ_a, ϕ_c and ϕ_i are separately determined. It is important that these methods give mutually consistent results [1,2]. In our theory, the basic quantity is the weight fraction of the a-domains defined by

$$w_a \equiv \bar{L}_a/(\bar{L}_a + \bar{L}_c + 2\bar{L}_i) = \xi/\chi. \tag{3.2}$$

Following Mandelkern [1,2], we assume that the densities of the c- and i-domain are almost the same, $\rho_c \approx \rho_i$, then, $\phi_c + \phi_i$ is rewritten as follows:

$$\phi_c + \phi_i \approx \frac{1/w_a - 1}{1/w_a - 1 + \rho_c/\rho_a} = \frac{\chi/\xi - 1}{\chi/\xi - 1 + \rho_c/\rho_a}. \tag{3.3}$$

Since χ is given as a function of ΔT by Eqs. (2.8) and (2.9), $\phi_c + \phi_i$ is a function of ΔT and ξ.

Extensive measurement of $\phi_c + \phi_i$ was done by Fatou and Mandelkern [24] for polyethylene using the delatometric method. In their work, fractionated polyethylene of M_η ranging from 3×10^3 to 1.55×10^6 are crystallized isothermally at $T_c = 130$ °C for 3–22 days and $\phi_c + \phi_i$ is measured by changing T very slowly (say, 0.5 °C per day). Some of their results are shown in Fig. 5. Since their samples are kept at each temperature for one day before measurement, the local-equilibrium between the a- and c-domains must be approximately established. Fig. 5 shows that $\phi_c + \phi_i$ decreases with increasing M_η. This is explained as follows [1,2]: as M_η increases, more and more LKs are trapped which obstruct crystallization and, as the result, $\phi_c + \phi_i$ decreases with increasing M_η. In our theory, this change is represented by trapping ratio ξ, which increases from zero to unity as M increases from zero to infinity. According to the theory, $\phi_c + \phi_i$ should decrease from unity to a limiting value, $(\chi - 1)/(\chi - 1 + \rho_c/\rho_a)$, as ξ increases from zero to unity (or M increases from zero to infinity). However, the experimental results (Fig. 5) show no tendency for $\phi_c + \phi_i$ to approach to a limiting value even at $M_\eta = 1.55 \times 10^6$. This seems strange, because $M_\eta = 1.55 \times 10^6$ must be already in the vicinity of $M \to \infty$ from the following reasons: (1) for $M > 10^5$, the lamellar thickness of polyethylene isothermally crystallized at $T_c = 130$ °C approaches to a limit value of ca. 700 (in CH_2 unit); (2) at $T_c = 130$ °C, sample $M_\eta = 1.55 \times 10^6$ takes $\phi_c + \phi_i = 0.38$, from which the average chain length per aici-sequence is estimated to be $\bar{L}_c + \bar{L}_a + 2\bar{L}_i \approx 2300$ ($\varphi_f = 0.2$ is assumed and $2\bar{L}_i$ is neglected); then, (3) each chain of $M_\eta = 1.55 \times 10^6$ contains 46 aici-sequences as an average or it goes in and out the lamellae ca. 46 times. Under such a condition, $M_\eta = 1.55 \times 10^6$ must be near the limit of $\xi \to 1$ while $\phi_c + \phi_i$ decreases as large as 0.03 as M_η changes from 1.47×10^6 to 1.55×10^6 and shows no tendency to approach a limit. This contradictory result is explained by possible existence of low-molecular-weight-components (LMWC) in the samples. To show this, we first note that ξ changes easily by a small amount of LMWC: suppose that a sample is composed of high-molecular-weight-component (HMWC) 1 with weight faction f_1 and LMWC 2 with weight faction f_2, $f_1 + f_2 = 1$, and assume that LKs formed by HMWC 1 alone are trapped completely while those formed by LMWC 2 alone or those formed between 1 and 2 are totally unknotted, then the trapping ratio of this sample is equal to $\xi = f_1^2$. If sample $M_\eta = 1.47 \times 10^6$ contains such LMWC, say, by $f_2 = 0.025$, the trapping ratio becomes $\xi = 0.95$ even if $M = 1.47 \times 10^6$ is large enough to give the limit $\xi \to 1$. If sample $M_\eta = 1.47 \times 10^6$ contains such amount of LMWC, while sample $M_\eta = 1.55 \times 10^6$ contains almost no LMWC, then their ξ should differ by $\Delta\xi = 0.05$, which is sufficient to explain the change of $\phi_c + \phi_i$ in Fig. 5. Since sample $M_\eta = 1.55 \times 10^6$ is the highest-molecular-weight residue of a column fractionation, it should contains only a trace of LMWC, while $M_\eta = 1.47 \times 10^6$ is an intermediate fraction which should contain a considerable amount of LMWC.[1]

From these considerations, we assume that sample $M_\eta = 1.55 \times 10^6$ is approximately in the limit of $M \to \infty$ and compare its $\phi_c + \phi_i$ with the theoretical curves for $\xi = 1$. At this point, however, another problem occurs: For polyethylene, two different values of T_m^0, 141.4 and 145.5 °C, are widely accepted and two possible values of conversion factor C, $C_c = 1.6$ and $C_e = 1.0$, exist (c.f. discussions in Section 2), thus, there are four possible theoretical curves for the four combinations of T_m^0 and C; $\phi_c + \phi_i$ is computed as function of T for these four combinations of T_m^0 and C and the results are shown in

[1] In a later work [25], it was found that $\phi_c + \phi_i$ of sample $M_\eta = 8 \times 10^6$ is less than that of $M_\eta = 1.55 \times 10^6$. However, $\phi_c + \phi_i$ ($= 1 - \lambda$ in their notation) of $M_\eta = 8 \times 10^6$ did not arrive at the local-equilibrium as evident from Figure 3 of Ref. [25], so that the equilibrium value of $\phi_c + \phi_i$ of sample $M_\eta = 8 \times 10^6$ should be larger than that reported by them.

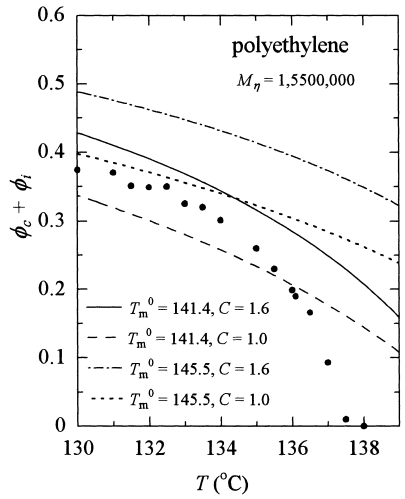

Fig. 6. Comparison of $\phi_c + \phi_i$ computed for $\xi = 1$ with experimental data of polyethylene $M_\eta = 155 \times 10^4$ (the same data as shown in Fig. 5). The theoretical curves are computed for four possible combinations of $T_m^0 =$ 141.1 or 145.5 °C and $C = 1.0$ or 1.6.

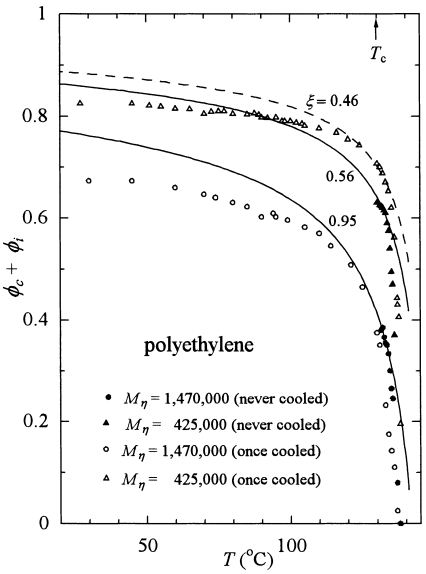

Fig. 7. Comparison of $\phi_c + \phi_i$ of polyethylene never cooled below T_c with those once cooled to the room temperature; $M_\eta = 42.5$ and 147×10^4. Data come form Ref. [24]. Experimental points are fitted at $T = 130$ °C with theoretical curves ($C = 1.25$) with ξ as an adjustable parameter.

Fig. 6. As seen from the figure, the slope of the experimental points (filled circles) for $M_\eta = 1.55 \times 10^6$ becomes steep suddenly around $T = 134$ °C, at which point melting begins (melting phenomena are discussed in Section 4); therefore, the theoretical curves should be compared with the points below $T = 134$ °C. The points for $T \leq 134$ come between the two theoretical curves for $T_m^0 = 141.4$ °C (the straight and broken line), while they come below the two theoretical curves for $T_m^0 = 145.5$ °C (the chain and dotted line). Considering that true experimental points for $\xi \rightarrow 1$ will come even below these points, $T_m^0 = 141.4$ °C seems to be more acceptable than $T_m^0 = 145.5$ °C. As for conversion factor C, it is difficult to say which of $C_c = 1.6$ and $C_e = 1.0$ is more favorable. As argued in the previous paper [19], we consider that N_c is more reasonable than N_e as the index of entanglement but this problem is still open to question. We must also consider possible errors in N_c (BF model) and N_e (BF model) determined in the previous work [18]. Although there remain these problems, we may conclude that the theoretical curves for $\xi = 1$ and $T_m^0 = 141.4$ °C agrees reasonably well with the experimental points for $M_\eta = 1.55 \times 10^6$. Considering the uncertainty of C for polyethylene, we had better treat it as an adjustable parameter for fitting; the best fitting for $M_\eta = 1.55 \times 10^6$ ($\xi = 1$, $T_m^0 = 141.4$ °C) is obtained at $C = 1.25$, which is hereafter used as the conversion factor for polyethylene. The result of fitting is shown in Fig. 5. Assuming $T_m^0 =$ 141.4 °C and $C = 1.25$, $\phi_c + \phi_i$ of the other samples are fitted by theoretical curves with ξ considering as fitting parameter. The results are shown in Fig. 5, in which ξ decreases continuously form $\xi = 1$ to 0.30 as M_η decreases from 1.55×10^6 to 4.7×10^4. In Fig. 5, the experimental points line on the theoretical curves in lower temperatures but, at temperatures where melting starts, they begin to deviate suddenly below the theoretical curves as expected.

The data shown in Figs. 5 and 6 are for the samples never cooled below $T_c = 130$ °C. Measurement was also done for samples once-cooled to the room temperature, after isothermal crystallization at $T_c = 130$ °C for 5–22 days, and then rising T very slowly for few weeks to the melting points; some of their data ($M_\eta = 4.25 \times 10^5$ and 1.47×10^6) are shown in Fig. 7 (open circles and triangles) together with the corresponding data for the never-cooled samples (filled circles and triangles, which are the same data as shown in Fig. 5); the theoretical curves fitted at $T_c = 130$ °C are also shown in the figure.

High molecular-weight sample, $M_\eta = 1.47 \times 10^6$. Roughly speaking, $\phi_c + \phi_i$ of the never-cooled sample agrees with that of the once-cooled sample. Since there is no data of the never-cooled sample below T_c, we cannot know how far $\phi_c + \phi_i$ of the two samples ($M_\eta = 1.47 \times 10^6$) agree with one another in the whole temperature range, but it is important that $\phi_c + \phi_i$ of the once-cooled sample almost returns to the value of the never-cooled sample around $T_c = 130$ °C; this means that no irreversible change occurred in $M_\eta = 1.47 \times 10^6$ by cooling below T_c. To making this point more clear, measurement of the never-cooled sample below T_c is necessary but, unfortunately, there is no such data in the literature. Since the experimental points for the never-cooled and once-cooled samples ($M_\eta = 1.47 \times 10^6$) agree roughly with one another in $110 \leq T \leq 135$, they should be almost in the local-equilibrium state and should agree reasonably with the theoretical curve as seen from Fig. 7. Outside of this temperature range, the experimental data deviate from the theoretical curve; the deviation for $T > 135$ is due to melting of the lamellae; the deviation in the low temperature region $T < 110$ may be a non-equilibrium

effect due to freezing of the sliding motion of the chains in the lamellae.

Low-molecular-weight sample, $M_\eta = 4.25 \times 10^5$. Its behavior is different from that of the high-molecular-weight sample, $M_\eta = 1.47 \times 10^6$. As seen from Fig. 7, $\phi_c + \phi_i$ of the once-cooled sample comes always above that of the never-cooled sample and the former does not return to the original value around $T_c = 130\,^\circ C$. This indicates that irreversible post-crystallization occurred in the once-cooled sample. This change may be due to the formation of crystallites in the a-domains, but it contradicts with the result that irreversible change does not occur in the high molecular-weight sample, which contains more a-domains. A natural explanation is that further unknotting of LKs occurs by cooling below T_c. If LKs are unknotted, ξ decreases and thus $\phi_c + \phi_i$ of the once-cooled sample will come above that of the never-cooled sample. The once-cooled data are fitted around $T_c = 130\,^\circ C$ by a theoretical curve with $\xi = 0.46$, which is smaller by 0.10 than that of the never-cooled sample $\xi = 0.56$; this means that ca. 18% of LKs remaining at the end of isothermal crystallization are further unknotted by cooling to the room temperature. Then, how it is possible to unknot LKs trapped in the a-sections without melting lamellae. If the lamellae do not melt, chain-ends must pass through the lamellae for LKs to be unknotted. Does each chain-end pass through the lamellae as shown in Fig. 8? If so, the velocity of unknotting should be linearly proportional to its concentration, or should be inversely proportional to M. In the present estimation, unknotting of LKs does not occur in $M_\eta = 1.47 \times 10^6$ (because the points of the once-cooled sample agree with or even come below those of the never-cooled sample as seen from Fig. 7), while a considerable amount (ca. 18%) of LKs is unknotted in $M_\eta = 4.25 \times 10^5$. This contradicts the above argument that the velocity of unknotting is inversely proportional to M, because M_η differs only by a factor three in these samples. This is an interesting problem but we cannot at present give a definite answer to it, because of the accuracy of the present estimation.

Limiting equilibrium amorphous content $\hat{w}_a^\infty(\tau)$. Above arguments are based on the assumption that sample $M_\eta = 1.55 \times 10^6$ is already in the limit $\xi \to 1$. To check this, the same experiment should be done for even higher molecular weight, narrow-distributed samples, which contain essentially no LMWC. By measuring $\phi_c + \phi_i$ of such samples, which are crystallized isothermally and then their temperature changed sufficiently slowly upward and downward from T_c (without once-cooled to the room temperature), we can know the T-dependence of local-equilibrium $\phi_c + \phi_i$ in the limit $\xi \to 1$. Theoretically, the equilibrium amorphous weight-fraction in the limit $\xi \to 1$ is a more fundamental quantity, which is hereafter called the 'limiting equilibrium amorphous ratio, $\hat{w}_a^\infty$' (∞ stands for $M \to \infty$ and $\wedge$, the local-equilibrium). Putting $\xi = 1$ in Eq. (2.4), we find

$$\hat{w}_a^\infty = 1/\chi. \tag{3.4}$$

Since χ is a function of T alone, so is $\hat{w}_a^\infty$; therefore, $\hat{w}_a^\infty$ is a specific function of each polymer. Considering that χ is given as a function of T by Eq. (2.9), it is a universal function of a reduced degree of supercooling

$$\tau = \frac{N_c \Delta h_m}{k_B T_m^0} \frac{\Delta T}{T}. \tag{3.5}$$

Now, we arrive at an important conclusion, limiting equilibrium amorphous ratio $\hat{w}_a^\infty(\tau)$ is a universal function of τ alone and it is independent of polymer species as well as thermal history and microscopic structure (such as $\bar{l}_a$, $\bar{l}_c$, φ_c, α, etc.) of the system. Once $\hat{w}_a^\infty(\tau)$ is determined for a polymer, we can compute $\hat{w}_a^\infty$ of any polymer at any temperature. Theoretically, average LK size L_{LK}^0 should be used for N_c on the rhs of Eq. (3.5) but N_c (or N_e) may be better from the experimental points of view. In any way, if the universality hypothesis of entanglement holds (i.e. if ratios among N_c, N_e and L_{LK}^0 are constant among polymers), we may use any of them to compute τ, because the result is the same except for the scale of τ. Using Eqs. (3.2) and (3.4), trapping ratio ξ is written as follows:

$$\xi = \hat{w}_a / \hat{w}_a^\infty \tag{3.6}$$

$$= \frac{1 + (\rho_c/\rho_a)(1/\hat{\phi}_a^\infty - 1)}{1 + (\rho_c/\rho_a)(1/\hat{\phi}_a - 1)}, \tag{3.7}$$

where $\hat{w}_a$ and $\hat{\phi}_a$ are the local-equilibrium values of w_a and ϕ_a. These equations can be used to determining ξ experimentally. In deriving Eq. (3.7), $\rho_c = \rho_i$ is assumed; therefore, Eq. (3.6) is more fundamental than Eq. (3.7). Although ξ has never been discussed in crystalline polymers, it is one of the most fundamental factors determining the structure of stacked lamellar crystals. It is, therefore, important that ξ of any sample (having any chemical structure, M, thermal history and crystallographic properties) can be determined purely experimentally by measuring $\hat{w}_a$ and using Eq. (3.6). It must be stressed that Eq. (3.6) depends on none of the details of the present theory except that $\chi(\tau)$ is independent of M or any crystallographic properties of the system, since it is determined in the catena networks; in this meaning, Eqs. (3.6) and (3.7) must come from a more general physical foundation.

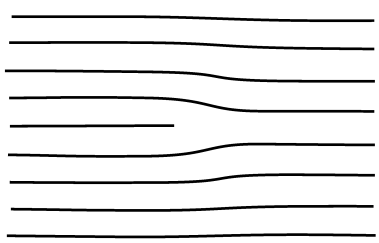

Fig. 8. An isolate chain-end in the lamella. Does this explain unknotting mechanism of LKs without melting the lamella?

Table 2
Surface energy σ_e of the stacking lamella crystals of polyethylene (computed for $T_m^0 = 145.5$ °C)

M_w	ζ (= $\bar{l}_c/\cos\alpha$) (in CH_2)[a]	T_m (°C)	ΔT_m	σ_e^{app} (erg/cm^2)[b]	ξ[c]	σ_e (erg/cm^2)					
						$\Delta T^{\otimes} = 0$[d]	4	8	12	16	20
12,500	470	136.2	9.3	172							
20,000	722	136.7	8.8	213							
38,000	625	137.0	8.5	219	0.30	195	189	184	178	174	169
47,000	906	137.2	8.3	311	0.31	275	266	257	250	243	236
56,000	720	137.2	8.3	254	0.31	227	219	213	206	201	195
56,000	1050	137.2	8.3	361	0.31	319	308	299	290	282	274
200,000	976	137.5	8.0	327	0.41	271	258	246	235	224	215
301,000	750	138.0	7.5	264	0.48	205	192	179	168	156	148
570,000	1100	139.0	6.5	375	0.63	236	206	178	153	130	109

Experimental data are given by Mandelkern et al. [28]; ξ and σ_e are not computed for $M_w = 12,500$ and 20,000, because the present theory cannot be applied to small ξ.

[a] ζ is the average lamella thickness (in the unit of CH_2) taken from Ref. [28, table 2]. $\bar{l}_c$ is related to ζ by $\bar{l}_c = \varsigma \cos\alpha$, where α is the tilt angle of the lamella. Although is not given in Ref. [28], it is not necessary in the present calculation of σ_e^{app} and σ_e; only experimental data of T_m and σ_e^{app} are used in the present calculation. ζ is shown here just for reference.

[b] σ_e^{app} (= σ_{ee} in the original symbol of Ref. [28]) is computed using average ζ (the values given in the fourth column of Table 3 in Ref. [28]). Their original data are given in cal/mol, which are converted into erg/cm^2 by multiplying factor 170/4600 suggested by the authors.

[c] Estimated by interpolation of ξs given in Fig. 5.

[d] $\Delta T^{\otimes} = T_c - T^{\otimes}$.

4. Melting point T_m and interfacial energy σ_e of lamellae

Interfacial energy σ_e is one of the most important parameters but its exact value is not known in stacked lamellar crystals. It is defined as the free energy per unit area of folding surface S and it is related to $\hat{\sigma}_e$ by

$$\sigma_e = \hat{\sigma}_e n \cos\alpha, \tag{4.1}$$

where n is the number of stems per unit area of S and α, the tilt angle. Experimentally, σ_e is determined by the relationship between lamellar thickness $\bar{l}_c$ and melting temperature T_m. It is given by condition $\Delta F(\chi, T_m) = 0$, which gives with the use of Eqs. (2.1), (2.7) and (4.1)

$$\Delta\mu_c(T_m) + \frac{\xi}{\chi - \xi}\Delta f_a(\chi) + \frac{2\sigma_e M_0}{\rho_c \bar{l}_c} = 0. \tag{4.2}$$

Usually, σ_e is determined by the Thompson–Gibbs equation,

$$T_m = (1 - 2\sigma_e M_0/\Delta h_m \rho_c \bar{l}_c) T_m^0, \tag{4.3}$$

which is obtained by neglecting the entanglement term (the second term) on the lhs of Eq. (4.2). Hereafter, the surface energy determined by Eq. (4.3) is called 'apparent surface energy σ_e^{app}',

$$\sigma_e^{app} = \rho_c \bar{l}_c^{obs} \Delta h_m \Delta T_m / 2 M_0 T_m^0, \tag{4.4}$$

where $\bar{l}_c^{obs}$ is the measured value of $\bar{l}_c$, which changes with the thermal history of the system.

It is well known that Eq. (4.4) gives a common value $\sigma_e \approx 90$ erg/cm^2 in many polyethylene crystals, such as single crystals, extended-chain crystals, etched or low molecular weight crystals, which contain no or small amount of a-domains [26]. However, it gives abnormally large σ_e^{app} in stacked lamellar crystals [27,28]. To see this, σ_e^{app} of isothermally crystallized polyethylene ($T_c = 130$ °C, $M_w = 1.25 \times 10^4 - 5.7 \times 10^5$) determined by Mandelkern et al. [28] are given in Table 2 (the fifth column). Their results show that σ_e^{app} increases with increasing M_w and, for $M_w = 5.7 \times 10^5$, it becomes more than four times the ordinary value of $\sigma_e \approx 90$ erg/cm^2. This abnormal result is explained by the entanglement term on the lhs of Eq. (4.2). To show this, experimental conditions must be considered carefully. In the most experiments, samples are crystallized at T_c, cooled once to the room temperature T_{room} where $\bar{l}_c^{obs}$ is measured and then T is elevated again to the melting point. In the cooling process, the samples will be frozen at a certain hypothetical local-equilibrium temperature $T^{\otimes}$ ($T_{room} \le T^{\otimes} \le T_c$), which is difficult to determine exactly. To avoid this difficulty, the samples should be kept for a sufficiently long time at the measuring temperature of $\bar{l}_c^{obs}$ and ξ, in order for the local-equilibrium to be established. In determining T_m, the temperature is usually elevated very fast, say 1–10 °C/min, so that $\bar{l}_c$, χ, Δf_a and ξ cannot follow the change of T and will remain in their measured values $\bar{l}_c^{\otimes} = \bar{l}_c(T^{\otimes})$, $\chi^{\otimes} = \chi(T^{\otimes})$, $\Delta f_a^{\otimes} = \Delta f_a(T^{\otimes})$ and $\xi^{\otimes}$, (note that, to establish the local equilibrium, it takes a very long time, say few weeks for polyethylene). To avoid the unnecessary changes of $\bar{l}_c^{\otimes}$, $\chi^{\otimes}$, $\Delta f_a^{\otimes}$ and $\xi^{\otimes}$, $T^{\otimes}$ should be chosen as close as T_m; the best way is to determine them at $T^{\otimes} = T_c$. If these conditions are satisfied, $\bar{l}_c$, χ, Δf_a and ξ on the rhs of Eq. (4.2) are equated to $\bar{l}_c^{\otimes}$, $\chi^{\otimes}$, $\Delta f_a^{\otimes}$ and $\xi^{\otimes}$, and ΔT_m, to the observed value $T_m^0 - T_m$ at the melting point; thus we find

$$\sigma_e = \left[1 - \frac{\xi^{\otimes}\Delta f_a^{\otimes} T_m^0}{(\chi^{\otimes} - \xi^{\otimes})\Delta h_m \Delta T_m}\right]\sigma_e^{app}, \tag{4.5}$$

Table 3
Surface energy σ_e of the stacking lamella crystals of polyethylene (computed for $T_m^0 = 141.4$ °C)

M_w	ΔT_m	σ_e^{app} (erg/cm^2)[a]	ξ	σ_e (erg/cm^2)					
				$\Delta T^{\otimes} = 0$[b]	4	8	12	16	20
38,000	4.4	113	0.30	96	89	83	78	73	69
47,000	4.2	157	0.31	131	121	112	104	97	90
56,000	4.2	129	0.31	107	100	92	86	80	72
56,000	4.2	183	0.31	152	141	131	122	113	105
200,000	3.9	159	0.41	119	104	91	79	68	58
301,000	3.4	120	0.48	77	62	49	36	25	15
570,000	2.4	138	0.63	35	1.6	−28	−55	−80	−103

Experimental data and ξ are the same as given in Table 2.
[a] σ_e^{app} is computed by the same method as in Table 2, except that $T_m^0 = 141.4$ °C is used.
[b] $\Delta T^{\otimes} = T_c - T^{\otimes}$.

where $\bar{l}_c^{obs} = \bar{l}_c^{\otimes}$ is assumed. In the definition of σ_e^{app} given by Eq. (4.3), the free energy of entanglement accumulated in the a-domains (the second term on the lhs of Eq. (4.2)) is formally included into σ_e^{app} so that it is always over-estimated than the true interfacial energy σ_e; Eq. (4.5) gives the correction for it.

To determine σ_e using Eq. (4.5), $\bar{l}_c^{\otimes}$, $\chi^{\otimes}$, $\Delta f_a^{\otimes}$ and $\xi^{\otimes}$ must be known but no such data is available in the literature. What we can do here is to show the effect of entanglement on σ_e^{app} using the experimental data given by Manderkern et al. [28] (Table 2). We first note that the samples given in Table 2 are prepared almost by the same methods as the once-cooled samples shown in Fig. 5 (they are both isothermal-crystallized at $T_c = 130$ °C for 20–40 days and then cooled to the room temperature); then, ξ of the former samples may be estimated by interpolating ξ of the latter; the results of the interpolation are given on the sixth column of Table 2. ξ thus estimated may be approximately equated to $\xi^{\otimes}$, since it changes only slightly in the cooling process. It is difficult to determine the frozen temperature $T^{\otimes}$ of these samples, because they are once cooled to the room temperature. If they were quenched rapidly to the room temperature, their $\bar{l}_c$, χ, ξ and Δf_a would be almost kept at their isothermal-crystallization values so that $T^{\otimes} \approx T_c$ may be assumed. Actually, the samples are cooled slowly for one day to the room temperature, so that $T^{\otimes}$ must be somewhere below T_c. However, the difference $\Delta T^{\otimes} = T_c - T^{\otimes}$ must be rather small, since the local-equilibration takes a much longer time, say, several weeks. Considering these points, σ_e is computed using Eq. (4.2), changing $\Delta T^{\otimes}$ between 0 and 20 degrees and the results are shown in the 7–12th column of Table 2. In this calculation, $T_m^0 = 145.5$ °C is assumed after Mandelkern et al. [28] As seen from Table 2, σ_e^{app} is always larger than σ_e, because the topological free energy accumulated in the a-domains is included in σ_e^{app}. The difference between σ_e^{app} and σ_e decreases with decreasing M_w and becomes almost negligible for $M_w < 10{,}000$; this is reasonable since trapping ratio ξ decreases with decreasing M_w so that the topological free energy accumulated in the a-domains becomes negligible. It is remarkable that a small change of $T^{\otimes}$ gives a large effect on the estimated value of σ_e particularly for large M_w; i.e. σ_e decreases with increasing $\Delta T^{\otimes}$, the change, mainly due to increase of $\Delta f_a^{\otimes} = \Delta f_a(T^{\otimes})$ with $\Delta T^{\otimes}$. Since $T^{\otimes}$ of the samples is not known, σ_e cannot be determined quantitatively, but we can say that (1) the entanglement term give a large effect on the estimated values of σ_e particularly for large M and (2) in contrast to σ_e^{app} found by Manderkern et al. [28], σ_e decreases with increasing M_w (in Table 2, σ_e increases once and then decrease as M_w increases, but it is not clear whether the initial increase is physically significant or just an artificial effect due to the errors in the estimated values or measurements).

There is another problem in determining σ_e. In the above calculation, $T_m^0 = 145.5$ °C is assumed after Manderkern et al. [28] but, if another popular value $T_m^0 = 141.4$ °C is chosen, a drastic change occurs. For $T_m^0 = 141.4$, σ_e is computed in the similar manner and given on the 5–10th column of Table 3, which shows that σ_e estimated for $T_m^0 = 141.4$ is much smaller than that for $T_m^0 = 145.5$. The difference, 4.1 °C, between the assumed values of T_m^0 gives large changes in ΔT_m, which eventually leads drastic decrease of σ_e and gives even negative values for the highest molecular weigh sample $M_w = 570{,}000$. Of course, negative values of σ_e are physically impossible; such a combination of $T^{\otimes}$ and T_m that makes σ_e negative is thermodynamically unstable and not realized. For $\Delta T^{\otimes} > 4.2$, σ_e of $M_w = 570{,}000$ becomes positive but the estimated values are much smaller than the ordinary values $\sigma_e = 90$ erg/cm^2. It is also remarkable that σ_e decreases rapidly with increase of M_w. Such a strong M-dependence of σ_e seems unreasonable, though the precise structure of the folding surface is not known well. The problem may be in the assumed value, $T_m^0 = 141.4$ °C. So long as the results in Tables 2 and 3 are considered, $T_m^0 = 145.5$ °C seems more acceptable than $T_m^0 = 141.4$ °C; this seemingly contradicts the argument in Section 3 that $T_m^0 = 141.4$ °C is more favorable to explain the behavior of $\phi_c + \phi_i$. However, the present calculations are not so accurate as to answer this difficult question, "which of $T_m^0 = 141.4$ °C and 145.5 °C is

right for polyethylene?" It should be discussed in a wider context, considering many other data simultaneously, so that it is out of the scope of this introductory work.

Although we cannot determine σ_e of the stacked lamellar crystals from the present calculations, we may at least conclude that the entanglement term gives a serious effect on its estimated value. To estimate it accurately, ξ and $\bar{l}_c$ should be determined at the isothermal crystallization temperature and T_m, by elevating T rapidly without once cooling to the room temperature. To calculate ξ using Eq. (3.6), $\hat{w}_a^{\infty}(\tau)$ must be determined in advance for narrow-distributed and UHMW samples. These conditions are partly and separately realized in some experiments but, unfortunately, the all necessary data ($\hat{w}_a(T_c)$, $\bar{l}_c(T_c)$ and T_m) are not given simultaneously. There is in principle no experimental difficulty in performing these experiments. It is, therefore, highly expected for them to be done, since σ_e is one of the most important parameters in crystalline polymers.

5. Microscopic structure of the system

Up to this point, we have considered bulk properties such as w_c and T_m. Now, we study how the microscopic structure such as thickness l_a and l_c of the a- and c-domains are determined. In the growing front of the lamellae, their thickness l_a^* and l_c^* are different from their matured values, l_a and l_c. Since the microscopic structure is determined primarily by l_a^* and l_c^*, we should first consider how they are determined in the crystallization process. Experimentally, l_c^* changes with $\Delta T_c = T_m^0 - T_c$ as follows

$$l_c^* = a/\Delta T_c + b, \tag{5.1}$$

where a and b are constant [3]. Various theories have been presented for the crystallization process of polymers [3]. Among them, the theory due to Lauritzen and Hoffman [29] is the most popular, which treats formation of the secondary nuclear of crystallization as reversible attachment of stems on the growing surface of the lamellae. In the recent theory of Sadler and Gilmer [30], reversible attachment of individual chain-elements is considered. These theories predict various features of crystallization, such T- and M-dependence of growth rate or surface roughening phenomena [3,29,30]. However, they are insufficient because they neglect entanglement in the nucleation process.[2] I believe that entanglement should play a central role also in this problem. Under this consideration, I have recently constructed a new theory of nucleation ('entanglement-fluctuation theory') based on LK model [22]. It will be, however, given in a separate paper [32], because it needs long and complicated discussions. In this paper, we consider the following more simple problem, "how l_a^* is determined for given l_c^*".

Here, it is assumed that l_c^* is given by the empirical Eq. (5.1) or by a certain theory, say, that will be given in the next paper [22,32]. Suppose that a secondary stable nuclear of width l_c^* is already formed on the growing surface and stems are attaching to step sites as shown in Fig. 9; this process is called 'step reaction.' For moderate supercooling ΔT_c (i.e. in the regime I and II of crystallization where the rate of the secondary nucleation is not very fast), chains are mostly crystallized by step reactions. The average feature of the a-sections is, therefore, determined by the step-reactions. There are three types of step reactions, in which tight-folds are formed (B) and (C) or not (A) as shown in Fig. 9. Let L_c^* be the frontier thickness (given in terms of chain-units) of the c-domain. The change of the free energy due to the step reactions are given by

$$L_a^*\Delta\mu_c^* + 2\hat{\sigma}_{nf}, \qquad \text{(reaction A)} \tag{5.2}$$

$$L_a^*\Delta\mu_c^* + 2\hat{\sigma}_f, \qquad \text{(reaction B)} \tag{5.3}$$

$$(1+n_f)L_a^*\Delta\mu_c^* + 2(\hat{\sigma}_{nf} + n_f\hat{\sigma}_f), \quad \text{(reaction C)} \tag{5.4}$$

where $\Delta\mu_c^*$ is the frontier value of $\Delta\mu_c$, $\hat{\sigma}_f$ and $\hat{\sigma}_{nf}$ are, respectively, the tight-folding and no-tight-folding interfacial energy per end of stems and n_f is the number of tight-folds formed in step reaction C (in Fig. 9(C), $n_f = 1$). Interfacial energy $\hat{\sigma}_e$ per the end of stems on the matured

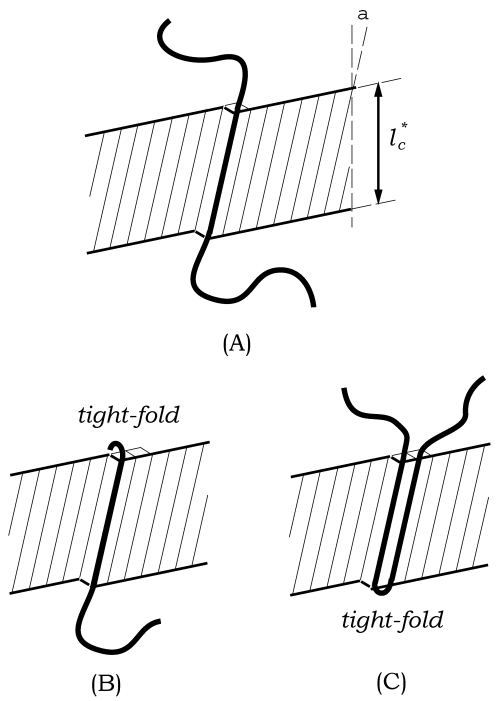

Fig. 9. Three types of step reactions. Tight-folds are formed in type B and C, but not in type A.

[2] In the later version of the Lauritzen–Hoffman theory [31], the reptation model is introduced to compute the velocity of reeling chains from melt. We consider that entanglement should a more central role than this in determining the size of nuclear as will be discussed in the next paper [22, 32].

folding surface is given in terms of $\hat{\sigma}_f$ and $\hat{\sigma}_{nf}$ by

$$\hat{\sigma}_e = \varphi_f \hat{\sigma}_f + (1 - \varphi_f)\hat{\sigma}_{nf} \tag{5.5}$$

where φ_f is the tight-folding ratio. Free energy change 5.2–5.4 represent the driving forces of the step reactions so that they are always negative. In the initial stage of crystallization of the chain, the step reactions occur rapidly because the topological repulsion among LKs is small (since concentration χ of LK is near the equilibrium value, $\chi = 1$). As crystallization proceeds, the topological repulsion increases with increasing χ and crystallization stops at a critical concentration, χ^*, where the topological repulsion surpasses driving force 5.2–5.4. This process is schematically shown in Fig. 10, in which LKs are represented by dots, the a-sections, by waving thin-lines and the c-section, by straight bold-lines.

Suppose that an a-section of length L_a is crystallizing by step reaction A as shown in Fig. 11 to form a c-section of length L_c^* and two a-sections of length L_a' and L_a'', $L_a = L_a' + L_a'' + L_c^*$. For simplicity, the i-sections are neglected, since the interfacial domains are small for moderate supercooling ΔT_c. It is also sufficient to consider step reaction A alone, because L_a^* is determined only by it as shown later. Let χ be the concentration of LK in the a-section before the reaction. The reaction occurs in such a manner that the newly formed a-sections have the same concentration,

$$\chi_1 = \chi L_a/(L_a - L_c^*). \tag{5.6}$$

The change of the topological free energy of LKs due to the reaction is given by

$$\Delta F_{LK}(L_a, L_c^*, \chi) = (L_a - L_c^*)\Delta f_a(\chi_1) - L_a \Delta f_a(\chi), \tag{5.7}$$

which is always positive, since χ increases by the step

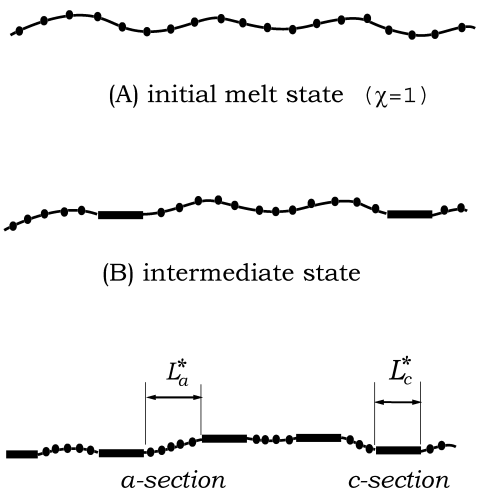

Fig. 10. As crystallization proceeds in a chain, χ increases from the topological equilibrium value $\chi = 1$ to final value $\chi^* > 1$. Bold and waving thin lines represent c- and a-sections, respectively, and dots, LKs trapped in the a-sections.

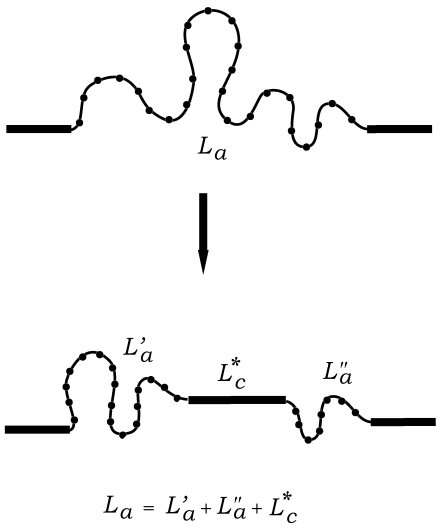

Fig. 11. When a step reaction A occurs in an a-section of length L_a, two new a-sections of length L_a' and L_a''. and a c-section of length L_c^* appear; $L_a = L_c^* + L_a' + L_a''$.

reaction. The net change of the free energy due to formation of the new c-section is given by the sum of $\Delta F_{LK}(L_a, L_c^*, \chi)$ plus the driving force of the step reaction, Eq. (5.2),

$$\Delta F(L_a, L_c^*, \chi) = \Delta F_{LK}(L_a, L_c^*, \chi) + L_c^* \Delta\mu_c^* + 2\hat{\sigma}_{nf}. \tag{5.8}$$

On the rhs of Eq. (5.8), $L_c^*\Delta\mu_c^* + 2\hat{\sigma}_{nf}$ is negative while $\Delta F_{LK}(L_a, L_c^*, \chi)$ is positive and nearly zero initially but increases with progress of crystallization of the chain. Thus, $\Delta F(L_a, L_c^*, \chi)$ is negative in the initial stage, where step reactions occur frequently. As crystallization proceeds, $\Delta F(La, Lc*, \chi)$ increases with increasing $\Delta F_{LK}(L_a, L_c^*, \chi)$ and crystallization stops when $\Delta F(L_a, L_c^*, \chi)$ becomes positive. Even if $\Delta F(L_a, L_c^*, \chi)$ becomes positive in shorter a-sections, it remains negative in longer a-sections, because $\Delta F_{LK}(L_a, L_c^*, \chi)$ decreases with increasing L_a. Therefore, the critical concentration χ^* at which crystallization of the chain finally stops is given by

$$\Delta F_{LK}(L_a^{*max}, L_c^*, \chi^*) + L_c^* \Delta\mu_c^* + 2\hat{\sigma}_{nf} = 0 \tag{5.9}$$

where L_a^{*max} is the maximum length of the a-sections in the growing frontier. Since the new c-section can be formed in any part of the a-section, L_a should distribute uniformly between 0 and L_a^{*max}; this means that the average length of the a-section just after finishing crystallization is given by

$$\bar{L}_a^* = L_a^{*max}/2. \tag{5.10}$$

Up to this point, we consider only step reaction A, neglecting formation of tight-folds by step reaction B and C (Fig. 9). B and C will not occur in the final stage of crystallization, because $\hat{\sigma}_f$ is larger than $\hat{\sigma}_{nf}$ so that driving force 5.3 and 5.4 for B and C are smaller than 5.2 for A. Tight-folds will be mainly formed in the initial stage of crystallization where $\Delta F(L_a, L_c^*, \chi)$ is still well negative. In the calculation of average length $\bar{L}_c^*$ of the c-section, however, the tight-folds should be counted. Considering that

$\bar{L}_c^*$ is the number average of L_c on the growing surface of lamellae, where tight-folding ratio φ_f should be the same as that in the matured lamellae, we find

$$\bar{L}_c^* = L_c^*/(1 - \varphi_f). \tag{5.11}$$

Now let us consider how final concentration χ^* is determined. We first note that χ is apt to be equalized in the chain due to the following three mechanisms: (1) step reactions occur more frequently in low χ sections than in high χ sections, (2) step reactions occur in such a manner that the newly formed a-sections have the same concentration given by Eq. (5.6) and (3) unbalance of χ in adjacent a-sections produces topological repulsive forces which make c-sections move along the chain in the direction to reduce the local unbalance of χ. Mechanism 1 levels off a long-scale distribution of χ, which is produced by unequal unknotting frequencies of LKs in the terminal and intermediate parts of the chains; i.e. unknotting of LKs occurs more frequently in the terminal parts than in the intermediate parts, so that χ apt to be smaller in the terminal than in the intermediate parts of the chain. The short-range fluctuation of χ is smoothed by all the three mechanisms. If all the a-sections of the chain have the same concentration χ^* at the end of crystallization, it is given by

$$\chi^* = \xi^*(\bar{L}_a^* + \bar{L}_c^*)/\bar{L}_a^*, \tag{5.12}$$

where $\bar{L}_a^*$ and $\bar{L}_c^*$ are the *number averages* of L_a^* and L_c^*, and χ^* is the trapping ratio of LK in the growing front. Generally, Eq. (5.12) gives certain average of χ^* over its distribution along the chain, but the effect of the distribution must be small since χ^* is apt be equalized by the above three mechanisms. Combining Eqs. (5.6)–(5.12), $\bar{L}_a^*$ is determined for given L_c^*. The average number of LKs trapped per a-section is given by

$$\bar{\nu}^* = \xi^*(\bar{L}_a^* + \bar{L}_c^*)/L_{LK}^0, \tag{5.13}$$

where L_{LK}^0 is the average chain length per LK in the equilibrium melt.

Now, χ^*, ξ^*, $\bar{\nu}^*$, $\bar{L}_a^*$ and $\bar{L}_c^*$ are all local values in the growing front. In some polymers, sliding motion of chains in the lamellae does not occur; in such polymers, their bulk values, χ, $\bar{L}_a$ and $\bar{L}_c$, are frozen at their frontier values, χ^*, $\bar{L}_a^*$ and $\bar{L}_c^*$. On the other hand, if the sliding motion occurs and the local-equilibrium is well established, they change toward their matured values, χ, ξ, $\bar{\nu}$, $\bar{L}_a$ and $\bar{L}_c$. However, the change of ξ^* and $\bar{\nu}^*$ must be small in long polymers, because, unknotting of LKs should occurs for them to change but it must be difficult once the chain is integrated into the lamellae. It may, therefore, be assumed

$$\xi \approx \xi^* \text{ and } \bar{\nu} \approx \bar{\nu}^*. \tag{5.14}$$

Of course, ξ and $\bar{\nu}$ change when the system is annealed for a sufficiently long time as discussed in Section 3, but their changes must be small in the crystallization process of very long chains as considered here. On the other hand, χ^* changes largely by annealing; its local-equilibrium value χ is determined by Eq. (2.9). The local-equilibrium values of $\bar{L}_a$ and $\bar{L}_c$ are given in terms of χ, ξ and $\bar{\nu}$ as follows:

$$\bar{L}_a = \bar{\nu} L_{LK}^0 \chi^{-1}, \tag{5.15}$$

$$\bar{L}_c = \bar{\nu} L_{LK}^0 (\xi^{-1} - \chi^{-1}), \tag{5.16}$$

The weight fraction of the a-domains is given by

$$w_a = \xi/\chi. \tag{5.17}$$

It is remarkable that w_c (or w_a), $\bar{L}_a$ and $\bar{L}_c$ are given in terms of entanglement-related quantities, χ, ξ, $\bar{\nu}$ and L_{LK}^0, alone (Eqs. (5.15)–(5.17)). Usually, the structure of stacked lamellar crystals is discussed in terms of w_c (or w_a), $\bar{L}_a$ and $\bar{L}_c$; in this meaning, *The structure of the stacked lamellar crystals is determined, macroscopically as well as microscopically, by entanglement*. Particularly, the bulk properties (w_a or w_c) are determined by χ and ξ alone, while the microscopic structure ($\bar{L}_a$ and $\bar{L}_c$) depends on extra parameter $\bar{\nu}$ or how LKs are partitioned in the a-sections. Since $\bar{\nu}$ is independent of χ and ξ, systems of the same crystallinity may have variety of microscopic structures according to how LKs are partitioned in the a-sections. Although these entanglement-related indices, χ, ξ and $\bar{\nu}$, have never been discussed before, they should play central roles in the stacked lamellar crystals.

Numerical calculations. As an example, numerical calculations are done for polyethylene. We assume that l_c^* is given by the empirical Eq. (5.1), which is rewritten in terms of the chain unit as follows

$$L_c^* = \kappa \hat{\sigma}_e T_m^0/\Delta h_m \Delta T_c + \delta L, \tag{5.18}$$

where κ and δL are constants. For a moderate ΔT_c, the second term δL may be neglected against the first term. Hoffman and Week [33,34] found that, in the early stage of crystallization, the plot of ΔT_m vs. ΔT_c (Hoffman–Weeks plot) shows often a straight line of slope 0.5; this means that κ is equal to ca. four in many systems.[3] Considering these points, we assume that δL is zero and κ, a constant near four. If $\Delta\mu_c^* = \Delta\mu_c$ is assumed, Eqs. (5.6), (5.9) and (5.12) are rewritten as follows:

$$(2\bar{L}_a^* - L_c^*)\Delta f_a(\chi_1^*) - 2\bar{L}_a^* \Delta f_a(\chi^*) = \kappa\hat{\sigma}_e - 2\hat{\sigma}_{nf}, \tag{5.19}$$

$$\chi^* = \xi^*[\bar{L}_a^* + L_a^*/(1 - \varphi_f)]/\bar{L}_a^*, \tag{5.19'}$$

$$\chi_1^* = 2\chi^* \bar{L}_a^*/(2\bar{L}_a^* - L_c^*). \tag{5.19''}$$

These equations determine $\bar{L}_a^*$ for a given L_c^* (assuming that φ_f and ξ^* are already given elsewhere). Once $\bar{L}_a^*$ is known, $\bar{\nu}$, $\bar{L}_a$ and $\bar{L}_c$ are computed by Eqs. (5.13)–(5.16), thus, we can know the microscopic structure of the system. Interfacial energy $\hat{\sigma}_e$ and $\hat{\sigma}_{nf}$ must be also given. We assume $\sigma_e = 90\ \text{erg/nm}^2$ for polyethylene. To convert σ_e into $\hat{\sigma}_e$ using Eq. (4.1), tilt angle α must be known but it is not usually given in the literatures. We may assume arbitrarily

[3] To get this result, Thompson–Gibbs Eq. (4.3) is assumed, which should hold approximately in the early stage of crystallization where condensation of LKs is still small.

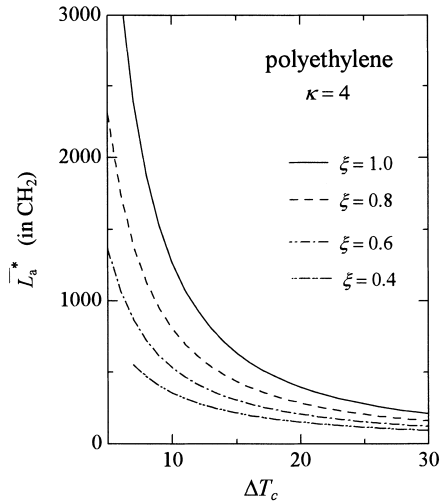

Fig. 12. Frontier a-domain thickness $\bar{L}_a^*$; ξ is changed between 0.4 and 1, κ fixed at four.

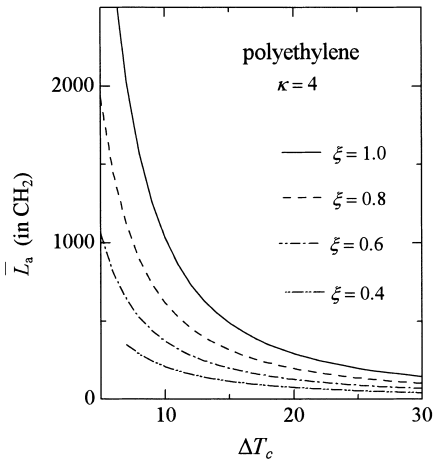

Fig. 13. Local-equilibrium a-domain thickness $\bar{L}_a$ computed at $T = T_c$; ξ is changed between 0.4 and 1, κ fixed at four.

$\alpha = 0$, because σ_e itself is not known well in stacked lamellar crystals (c.f. discussion in Section 4) so that it is not worth discussing the accuracy of α assumed. Non-tight-folding interfacial energy $\hat{\sigma}_{nf}$ is also not known, but its value gives no serious effect on the rhs of Eq. (5.19), because $\hat{\sigma}_{nf}$ must be considerably smaller than $\hat{\sigma}_e$; therefore, we assume arbitrarily $\hat{\sigma}_{nf} = 0.5\hat{\sigma}_e$. In this work, κ is treated as sole adjustable parameter ($2.4 \leq \kappa \leq 6$) and uncertainties in α, $\hat{\sigma}_e$ and $\hat{\sigma}_{nf}$ assumed are formally included in the change of κ, (theoretically, κ should be determined in the nucleation process on the growing surface of lamellae; this problem will be discussed in the next paper.[4] Tight-folding ratio φ_f, which appears on the rhs of Eq. (5.19a), give a considerable effect on $\bar{\nu}$, $\bar{L}_a^*$, $\bar{L}_a$ and $\bar{L}_c$ but it changes only slightly ordinary observable quantities such as w_c, $\bar{l}_a$ and $\bar{l}_c$; in this work, therefore, we assume arbitrarily $\varphi_f = 0.3$. If Eq. (5.5) holds, $\hat{\sigma}_e$ must depend on φ_f but such a change of $\hat{\sigma}_e$ is also formally included in the change of κ. Trapping ratio ξ^* ($\approx \xi$ assumed) should be determined in the frame of our theories but, at present, it is considered as a variable parameter.

The numerical calculations are done changing ΔT_c and ξ in range $5 \leq \Delta T_c \leq 30$ and $0.4 \leq \xi \leq 1$; region $\xi < 0.4$ is omitted because the present theory cannot be applied to small ξ; region $\Delta T_c < 5$ is omitted because the numerical calculation become unreliable. Parameter κ is changed in range $2.4 \leq \kappa \leq 6$, but the most calculations are done for its most probable value, $\kappa = 4$. The results of the calculations are summarized as follows:

(1) *Behaviors of* $\bar{L}_a^*$, $\bar{L}_a$ *and* $\bar{L}_c$. In Figs. 12–14, $\bar{L}_a^*$, $\bar{L}_a$ and $\bar{L}_c$ are plotted against ΔT_c, changing ξ (κ fixed at four). Roughly speaking, these quantities behave like $1/\Delta T_c$; this comes from the similar ΔT_c-dependence of L_c^* given by Eq. (5.18) (in which $L = 0$ is assumed). However, ξ-dependence of $\bar{L}_a^*$ and $\bar{L}_a$ are quite different from that of $\bar{L}_c^*$ and $\bar{L}_c$: $\bar{L}_c^*$ is independent of ξ by definition and $\bar{L}_c$ changes only slightly with ξ (Fig. 14), while $\bar{L}_a^*$ and $\bar{L}_a$ decrease rapidly with decreasing ξ (Figs. 12 and 13). This result is reasonable, because $\bar{L}_c^*$ and $\bar{L}_c$ are primarily determined by the secondary nuclear size, which should be independent of ξ, while the amount of a-domains is determined by the number of LKs trapped in the a-domains. To see the effect of parameter κ, $\bar{L}_a^*$ is plotted against ΔT_c changing κ (ξ fixed at unity) in Fig. 15, which shows that $\bar{L}_a^*$ is almost independent of κ; this is in contrast to the behavior of L_c^*, which changes linearly proportional to κ (c.f. Eq. (5.18) $\delta L = 0$ assumed).

(2) *Average number of trapped LKs per a-section* $\bar{\nu}$. It is plotted against ΔT_c changing in ξ Fig. 16. $\bar{\nu}$ behaves almost like $\bar{L}_a^*$ except for their scales; it change like $1/\Delta T_c$ and decreases rapidly with decreasing ξ. It is important that $\bar{\nu}$ is considerably larger than unity; if $\bar{\nu}$ were less than unity, the present theory would become insignificant.

(3) *Ratio* $\bar{l}_c/\bar{l}_c^*$. By annealing, the thickness of the

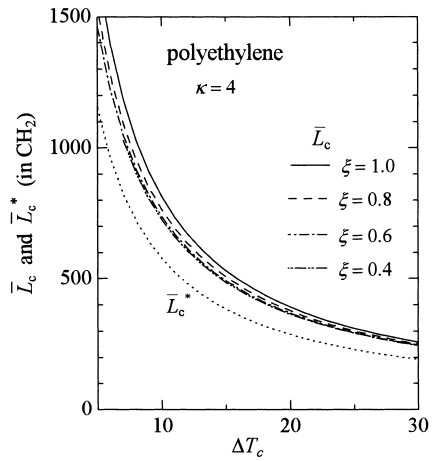

Fig. 14. Local-equilibrium c-domain thickness $\bar{L}_c$ computed at $T = T_c$; ξ is changed between 0.4 and 1, κ fixed at four. For refreference, frontier c-domain thickness L_c^* is shown by dotted line.

[4] According to the early works of Strobl et al. [4,5] this sample should contain interfacial domains of $\bar{l}_i = 0.5–1.4$ nm, [4] which are further divided into crystalline-like and amorphous-like transition regions [5]. These regions should give considerable effects on $\phi_c + \phi_i$, $\bar{l}_a$ and $\bar{l}_c$ but they are neglected in the present introductory work.

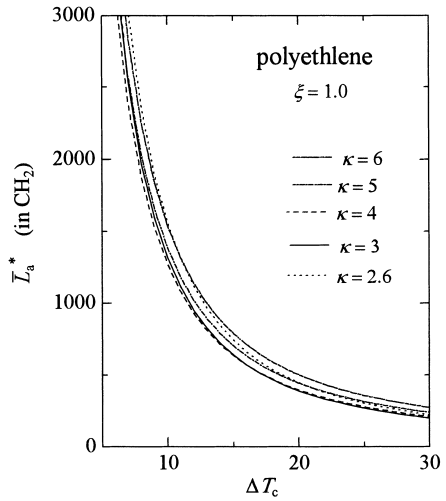

Fig. 15. Frontier a-domain thickness $\bar{L}_a^*$; κ is changed between 2.6 and 6, ξ fixed at unity.

c-domains increases while that of the a-domains decreases so that the growing fronts of the lamellae have a trapezoid form as shown in Fig. 17; this means $\bar{L}_a^* > \bar{L}_a$ and $\bar{L}_c^* < \bar{L}_c$, which are seen from Figs. 12–14. In Fig. 18, ratio $\bar{l}_c/\bar{l}_c^*$ $(= \bar{L}_c/\bar{L}_c^*)$ is plotted against ΔT_c (only the result for $\xi = 1$ is given, since $\bar{l}_c/\bar{l}_c^*$ is almost independent of ξ). For $\kappa = 4$, ratio $\bar{l}_c/\bar{l}_c^*$ is roughly constant near 1.4. However, $\bar{l}_c/\bar{l}_c^*$ increases considerably with decreasing κ (Fig. 17).

(4) *Condensation ratio χ^* and χ*. They are plotted against ΔT_c in Fig. 19. As argued in Section 3, χ is a specific function of T and it is independent of any other crystallographic properties of the system. On the other hand, χ^* decreases largely with decreasing ξ (or decreasing M). For small ξ, χ^* is near the melt value, $\chi = 1$, thus almost no condensation of LKs occurs in the growing front of short polymers. As ξ increases, χ^* increases to a considerable value, say, $\chi^* = 1.5$, so that considerable condensation occurs in the growing front of long polymers. This difference may explain the change of morphology (say,

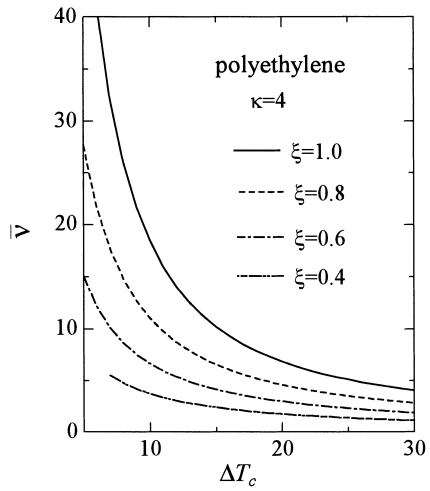

Fig. 16. Average number of LKs trapped per a-section; ξ is changed between 0.4 and 1, κ fixed at four.

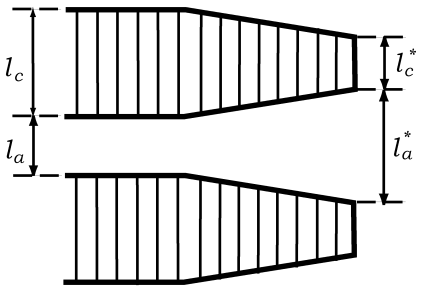

Fig. 17. A trapezoid form of the growing front of lamella.

the transition from spherulite to axialite) with increasing M observed in experiments [3]. It is also important that χ^* is considerably smaller than its matured value χ (Fig. 19); this means that there is a steep gradient of chemical potential $\Delta\mu_a$ near the growing front of the a-domains (see Fig. 18). Since the topological repulsive force among LKs is larger than or similar, in magnitudes, to the driving force of crystallization, $L_c\Delta\mu_c$, or surface tension $\hat{\sigma}_e$, the M-dependence of χ^* and the gradient of $\Delta\mu_a$ in the growing front should give large effects on the growth mechanism, although such a effect has never been discussed. These problems will be discussed in future works.[5]

Comparison with experiments. T-dependence of $\bar{l}_a$ is studied by Albrecht and Strobl (AS) for polyethylene using small-angle X-ray scattering [6]. Trapping ratio ξ of their sample (BASF Lupolen 6011L isothermally crystallized at $T_c = 124$ °C) is determined from T-dependence of $\phi_c + \phi_i$ $(= \omega_c$ in their notation) as shown in Fig. 20, in which the experimental data read from Fig. 8 of their paper [6] are fitted with a theoretical curve of $\xi = 0.51$ $(C = 1.25$ assumed as discussed in Section 3). Fig. 20 is similar to that of Fatou and Mandelkern's [24] shown in Fig. 7; in both figures, experimental points deviate below the theoretical curves for $T < 110$ °C, where the sliding motion of chains in lamellae is slowed down. Lamellar thickness $\bar{l}_c$ is not given in AS's paper [6], but it is estimated from their early work [4] in which the same experiments are done using the same sample (BASF Lupolen 6011L); from heating curves of $\bar{l}_c$ crystallized at $T_c = 125$ and 127 °C (Fig. 8 of Ref. [4]), $\bar{l}_c$ (crystallized at $T_c = 124$ °C) is estimated to be $\bar{l}_c \approx 28$ nm at $T = 124$ °C. From Fig. 14, $\bar{L}_c$ is estimated to be 320 $[CH_2]$ at $\xi = 0.51$ and $\Delta T_c = 21.5$; it is converted into lamellar thickness $\bar{l}_c = 34.7$ nm, which is near the experimental value, 28 nm. In our theory, $\bar{l}_c$ is primarily determined by nuclear size l_c^*, which is given by the empirical Eq. (5.1). Particularly in this work, κ on the rhs of Eq. (5.18) is treated as a main adjustable parameter determining l_c^* or, more simply, as a sole adjustable parameter to fit $\bar{l}_c$ to the experiment, (note that observable quantities, $\phi_c + \phi_i$, $\bar{l}_a$ and $\bar{l}_c$, depend only weakly on tight-folding ratio φ_f and tilt angle α, so that it is not worth discussing the accuracy of their assumed values $\varphi_f = 0.3$

[5] Some of these problems have been discussed in the annual meetings of the polymer society of Japan [21,23].

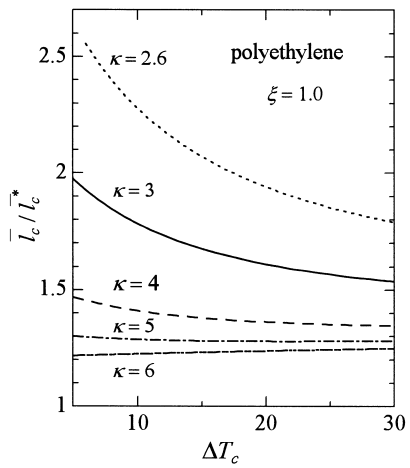

Fig. 18. Ratio $\bar{l}_c/\bar{l}_c^*$ computed for various κ; ξ fixed at unity.

and $\alpha = 0$; their changes are formally included in the variation of κ). The best fit of $\bar{l}_c$ is obtained at $\kappa = 2.99$, which is in the acceptable range from the most probable value, $\kappa = 4$. In Fig. 21, T-dependence of $\bar{l}_a$ determined by Albrecht and Strobl [6] is shown by open circles (cooling process) and filled circles (heating process); a theoretical curve computed for $\xi = 0.51$ and $\kappa = 2.99$ is shown by a bold line, which deviates ca. 1.5 nm above the experimental points but its T-dependence agrees well with the experiment. The deviation may be due to neglecting the interfacial domains in the present calculation.[2]

AS argued that $\bar{l}_a(T)$ is almost independent of the crystallization condition [6]. According to Eq. (5.15), $\bar{L}_a$ is determined by χ and $\bar{\nu}$, among which χ is a universal function of T, while $\bar{\nu}$ is almost independent of T, if assumption $\bar{\nu} \approx \bar{\nu}^*$ and $\xi \approx \xi^*$ hold. In our theory, $\bar{\nu}$ (strictly speaking $\bar{\nu}^*$) is determined in the growing process of lamellae so that it changes with T_c and ξ^* ($\approx \xi$) as shown in Fig. 16. Thus, $\bar{L}_a$ has a common T-dependence determined by $\chi(T)$ but its magnitude is determined by $\bar{\nu}$, which changes with the crystallization condition in contrast to AS's

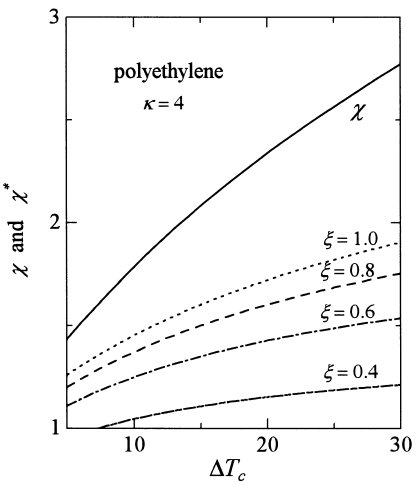

Fig. 19. Condensation ratio of LKs in the equilibrium a-domains, χ, and in the growing front, χ^*.

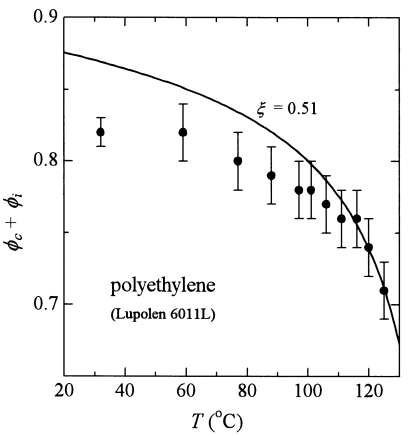

Fig. 20. Crystallinity $\phi_c + \phi_i$ of polyethylene (Lupolen 6011L, $T_c = 124$ °C) measured by Albrecht and Strobl [6]. Data are read from Fig. 8 of their paper [6]. Experimental points are fitted by theoretical cure for $\xi = 0.51$, $\kappa = 2.99$ and $C = 1.25$.

argument [6]. However, $\bar{\nu}$ changes only slightly for a small variation of T_c; for example, if T_c changes from 124 to 125 °C, $\bar{\nu}$ changes from 2.695 to 2.833 (ξ is fixed at 0.51) or $\bar{L}_a$ (and hence $\bar{l}_a$) increases only by 5%, which is almost within the experimental error. AS considered that $\bar{l}_a$ is a common function of T by comparing $\bar{l}_a$ vs. T curves of samples crystallized at $T_c = 124$, 125 and < 124 °C (Fig. 10 in their paper [6]); looking at their picture closely, however, the curves have a common T-dependence but seem to dislocate a little vertically. Strictly, their results should be interpreted that $\bar{l}_a$ has a common T-dependence and its magnitude changes only slightly with the crystallization conditions; this is consistent with our results. In our theory, $\bar{\nu}(T_c, \xi)$ increases monotonically with increasing T_c as shown in Fig. 16, but $\bar{l}_a$ seems change irregularly with T_c in AS's experiment (Fig. 10 of their paper [6]); this may be explained that ξ also changes with the crystallization condition. However, the shifts are too small to give a definite answer. Further experiments changing M and T_c wildly are expected.

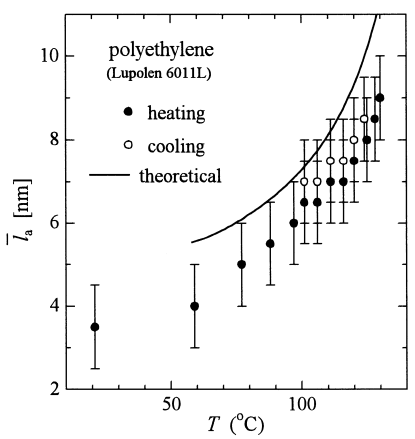

Fig. 21. T-dependence of a-domain thickness $\bar{l}_a$ measured by Albrecht and Strobl for polyethylene (Lupolen 6011L, $T_c = 124$ °C) [6]. The theoretical curve is computed for $\xi = 0.51$, $\kappa = 2.99$ and $C = 1.25$.

6. Concluding remarks

The purpose of this work is to give a grand scope of the roles of entanglement in crystalline polymers. The essential point of our theory is that structure of semi-crystalline polymers (such as w_c, $\bar{L}_a$ and $\bar{L}_c$) is determined by three variables due to entanglement, condensation ratio χ, trapping ratio ξ and average number $\bar{\nu}$ of LKs trapped per strand in a-domains, which have never been discussed before. It is shown that $\chi(=1/\hat{w}_a^{\infty})$ is a universal function of the reduced temperature, $\tau=(N_c\Delta h_m/k_B T_m^0)\Delta T/T$, which is common for the all polymers including simulation models. Thermodynamically, $V/V_0=1/\chi(\tau)$ represents the reduced equation of state of LK, where V is the volume of the a-domain (or of a catena network considered in the previous work [17]) and V_0 is the volume in the topological equilibrium state; this is an analogy of the reduced equation of state of gasses, in which T, V and P are reduced by their triple point values. The universality nature of $\chi(\tau)$ is observed in Arbrecht and Storobl's experiment [4,6] in which $\bar{l}_a(T)$ has a common T-dependence independent of the crystallization condition. If reduced temperature τ is used for T, $\bar{l}_a(\tau)$ should have a common τ-dependence independent of polymer spices. Theoretically, $\chi(\tau)$ is computed by simulation of catena networks independently of crystalline polymers [17]. Experimentally, χ $(=1/\hat{w}_a^{\infty})$ is determined from equilibrium crystallinity, say, $\phi_c+\phi_i$ of polyethylene measured by Fatou and Manderkern [24], assuming that their highest molecular-weight sample ($M_\eta=1.55\times10^6$) is in the limit $M\to\infty$. To know the precise functional form of $\chi(\tau)=1/\hat{w}_a^{\infty}(\tau)$ is important in the study of crystalline polymers as well as of entanglement. Measurement of $\hat{w}_a^{\infty}$ is necessary to know an empirical equation of state of LK. In semi-crystalline polymers, $\hat{w}_a^{\infty}$ is used to determining the trapping ratio ξ using Eq. (3.6). It is, therefore, highly expected for Fatou and Manderkern's experiments [24] to be done using more high molecular weight and narrow-distributed samples.

Another important finding is that the topological free energy of entanglement accumulated in a-domains gives a serious effect on the melting phenomena of stacked lamellar crystals. Particularly, interfacial energy σ_e changes largely from that determined by the usual Thompson–Gibbs equation. The problem is that the effect of freezing temperature $T^{\otimes}$ has not been considered well in melting experiments, because lamellar thickness $\bar{l}_c$ changes only slightly with a small change of $T^{\otimes}$. However, the topological free energy depends strongly on $T^{\otimes}$ and even a slight change of $T^{\otimes}$ gives a large effect on σ_e as shown in Tables 2 and 3. To solve this problem, samples should be equilibrated at $T^{\otimes}$ as close as possible to T_m for a sufficiently long time and, then, the temperature should be changed rapidly to T_m so that $T^{\otimes}$ is kept constant. It is a serious problem that a precise value of σ_e in stacked lamellar crystals is not known. Is it different from its ordinary value 90 erg/cm^2 or does it change with tight-folding ratio φ_f as Eq. (5.5) suggests? For quantitative comparison of the theory with experiments, σ_e must be known accurately. For this purpose, further experiments are expected which are applicable to Eq. (4.5). Since Eq. (4.5) contains trapping ratio ξ, $\hat{w}_a^{\infty}(\tau)$ must be known first to determine σ_e. Precise determination of $\hat{w}_a^{\infty}(\tau)=1/\chi(\tau)$ is, therefore, the first step to the all entanglement problems.

In Fig. 21, $\bar{l}_a(T)$ agrees fairly well with the experiments of Albrecht and Strobl [6] but, in principle, it should agree almost exactly if the interfacial domains are considered, because χ, ξ and $\bar{\nu}$ are determined to fit experiments. In the present work, ξ was determined for crystallinity $\phi_c+\phi_i$ to agree with the experiment; parameter κ (c.f. Eq. (5.18)), which determines $\bar{\nu}$, was adjusted for lamellar thickness $\bar{l}_c$ to agree with the experiment; parameter C (c.f. Eq. (2.5) and (2.5′)) is adjusted for $1/\chi(\tau)$ to agree with experimental $\hat{w}_a^{\infty}(\tau)$. Therefore, the agreement shown in Fig. 21 is almost a matter of course, although it shows that the theory is self-consistent. The important point is that these agreements are obtained for reasonable values of the parameters, $C=1.25$ and $\kappa=2.99$ for polyethylene. This indicates that we are going on a right way, although further improvements in regard to interfacial domains and chain-end effects are necessary for quantitative discussions. Among these parameters, C is a matter of pure entanglement problems: It should be studied in the context of universality of entanglement, where it is discussed which of n_c, N_e, N_e^*, L_{LK}^0, etc. is the most appropriate parameter of entanglement [18,19]; this problem is now under investigation and will be answered soon. In this work, κ is treated as an adjustable parameter, but it should be determined in the theory of nucleation which will be presented in the next paper [22,32]. Theoretically, ξ is determined how LKs are unknotted in the process of crystallization so that it is a kind of chain-end effects which are neglected in the present work; this problem will be studied in future works.

The present work is an introduction to the topological theory of crystalline polymers, in which such problems as (1)–(4) stated in the beginning have been studied [20–23]. Beside them, there are many problems, such as unknotting of LKs during crystallization and annealing, surface-roughening phenomena, memory of crystal after melting, single crystal formation in dilute solutions, formation of super structures (such as spherulite or axialite), stress crystallization, fiber crystal formation by drawing and so on, in which entanglement will play important roles. They are also our future problems.

Acknowledgements

I acknowledge professor Masamichi Hikosaka of Hiroshima University for his advices and discussions on this work. I also acknowledge support from a Grant-in-aid for Scientific Research from the Ministry of Education, Science and Culture, Japan (No. 07651100).

References

[1] Manderkern L. In: Dosiere M, editor. Crystallization of polymers. The Netherlands: Kluwer; 1993. p. 25–37.
[2] Manderkern L. Acc Chem Res 1990;23:380.
[3] Gedde UW. Polymer physics. London: Kluwer; 1999. Chapter 7–9.
[4] Tanabe Y, Strobl GR, Fischer EW. Polymer 1986;27:1147.
[5] Mutter R, Stille W, Strobl G. J Polym Sci, Polym Phys 1993;31: 99.
[6] Albrecht T, Strobl G. Macromolecules 1995;28:5827.
[7] Fisher EW. Kolloid Z Z Polym 1967;218:97.
[8] Mansfield ML. Macromolecules 1982;20:1384.
[9] Riger J, Mansfield ML. Macromolecules 1989;22:3810.
[10] Smith P, Lemstra PJ. Makromol Chem 1979;180:2983.
[11] Smith P, Lemstra PJ, Pijpers JPL, Kiel AM. Colloid Polym Sci 1981; 259:1070.
[12] Doi M, Edwards SF. The theory of polymer dynamics. Oxford: Clarendon Press; 1986.
[13] Iwata K, Edwards SF. Macromolecules 1988;21:2901.
[14] Iwata K, Edwards SF. J Chem Phys 1989;90:4567.
[15] Iwata K. Macromolecules 1991;24:1107.
[16] Iwata K, Tanaka M. J Phys Chem 1992;96:4100.
[17] Iwata K, Tanaka M, Yako M, Kohno Y. Polymer 2002; 43.
[18] Tanaka M, Iwata K, Kohno M, Kuzuu S. J Theor Comput Polym Sci 2000;10:299.
[19] Tanaka M, Kuzuu S, Iwata K. J Theor Comput Polym Sci 2000;10: 309.
[20] Iwata K, Yako M, Tanaka M. Polym Prepr Jpn 1999;48:3727.
[21] Iwata K. Polym Prepr Jpn 2000;49:2652.
[22] Iwata K. Polym Prepr Jpn 2001;50:1695.
[23] Iwata K. Polym Prepr Jpn 2001;50:1697.
[24] Fatou JG, Mandelkern L. J Phys Chem 1960;.
[25] Ergoz E, Fatou JG, Mandelkern L. Macromolecules 1972;2:147.
[26] Wunderlich B, Czornyj G. Macromolecules 1977;10:906.
[27] Schultz JM, Robinson WH. Bull Am Phys Soc 1965;10:67.
[28] Mandelkern L, Price JM, Gopalan M, Fatou JG. J Polym Sci Part A-2 1966;4:385.
[29] Lauritzen JI, Hoffman JD. J Res Nat Bureau Std A Phys Chem 1960; 64A:72.
[30] Sadler DM, Gilmer GH. Polymer 1984;25:1446.
[31] Hoffman JD, Miller RI. Macromolecules 1988;21:3038.
[32] Iwata, K, in preparation.
[33] Hoffman JD, Weeks JJ. J Chem Phys 1965;42:4301.
[34] Weeks JJ. J Res Nat Bur Std (US) 1963;67A:441.